Response to Reviewer #1 Comments
Kurt Imhoff
Andrew Wilcox

---

(1). As discussed in the introduction (p 1512), in section 4 (p 1526) and exemplified by figure 1, the sudden increase of discharge at the confluence is likely to be a important control parameter of sediment dispersion and transport distances. It is therefore regrettable that the sites being ungauged, the entire analysis relies on water stage measurements. This weakens the conclusions of the paper.

We certainly agree that discharge measurements are valuable for this (or really any) type of fluvial process study, but we do not agree that stage measurements weaken our conclusions; we consider these a suitable substitute, complemented by topography measurements, for understanding differences in the hydrologic driving forces temporally (across the hydrograph) and spatially (among study sites), for our study purposes. Our use of stage data is supported by Phillips et al. (2013), who found that stage is an acceptable metric for calculating I, which has been shown to be analogous to the time above the critical discharge threshold for motion. Direct measurement of discharge across the hydrograph at our five sites was also not feasible, and gauged headwater streams of the type we target here are not available in our region.*

(2). Abstract, page 1520, line 14-15. The authors mention the existence of "finer grained experiments" in which efficient transport corridors are also observed. Unless I'm wrong, these "finer-grained experiments" are discussed nowhere in the manuscript.

We have changed "finer grained" to "prior"- our intention was to allude to prior studies involving finer-grained particles, but we agree that this was not clear.

Line 20

Within the confluence zone, transport occurs along scour hole margins in narrow, efficient transport corridors that mirror those observed in ~~finer-grained~~ prior experiments and field studies.

(3). page 1514, line 5. What exactly do you call a "disturbance"? Please be more explicit.

In this case, we are referring to physical disturbances that disrupt equilibria among transport capacity, sediment supply, and channel morphology, including the confluence morphology discussed (scour hole with flanking bars) via sediment evacuation or infilling. Such disturbances can include floods and debris flows; in our study system post-wildfire debris flows are a key disturbance.

Line 131

We selected a study area in the East Fork Bitterroot (EFB) River basin in western Montana, USA (Fig. 2) that is typical of semiarid, snowmelt-dominated, montane headwater systems. This location lacks ~~lacking~~ recent physical disturbances ~~affecting the sediment equilibrium~~ (~~i.e.,~~e.g., post-wildfire debris flows) and contain~~sing~~s confluences exhibiting characteristics of the equilibrium morphology described above.

(4). page 1515, lines 25-30. What is the bed D50? What is the D50 of the tracer particles?

Grain size information for the bed and tracers are provided in Tables 1 and 2, respectively. We have revised the text, including additional references here to Tables 1 and 2, to improve clarity.

Line 187

~~**30mm long were drilled using a ~ 0.8mm diamond-tipped drill bit.**~~**….** ~~**Tracer particles used were primarily larger than the bed *D*50 (Table 1), as particles with b axis below 45mm often fractured during drilling.**~~ **We tagged cobbles with median axes mostly between 60 and 130mm (Fig. ~~3~~4, Table 2). Many of the tracer particles were larger than the bed *D*50 (Table 1), because particles with b axis below 45mm often fractured during drilling.** ~~**This represents the *D*37 to *D*70 size fraction, which w**~~**We assumed our tracer particles, which fell within the *D*37 to *D*70 size fraction of bed materials, to be representative of the coarser fraction of mobile bedload particles.** ~~**The D50 of our tagged tracers varied between 0.077m and 0.082m (Table 2).**~~ **The results and interpretation of our sediment tracers thus do not apply for the entire mobile bedload population in this system.**

(5). page 1516, lines 16-19. How exactly did you make sure that the tracer particles were deposited randomly? Why would randomly distributed particles be more likely to move to natural positions? How long does it take? And what do you mean by “natural position”? I understand that your objective is to minimize the possible influence of the initial condition. But your statements need to be supported by observations or reasoning. For my part, I would be inclined to believe that it is very difficult to ensure a random distribution on the field so that starting from a regular grid is the most reproducible initial condition even though it is not the most “natural” one (as in Phillips et al. 2013).

We have revised the text here to address these comments. We have deleted the word “random” to describe the grid and replaced it with reference to Figure 5, which shows the initial layout of our tracer particles. We have also deleted the second part of the sentence (where we referred to “natural position”). We have added text recognizing the challenge of simulating natural particle arrangement in tracer deployment, per the reviewer’s comment. The new text reads:

Line 209

Our seeding method emulated that employed by Ferguson and Wathen (1998): particles were seeded loosely on the bed surface near the channel thalweg in a ~~**random**~~ **grid (Fig. 5).**~~**, an established and easily reproducible initial condition for coarse particle tracers.**~~ **Mimicking the arrangement of fluvially deposited gravels and minimizing the influence of the initial condition of particle deployment is a challenge in tracer studies, but a regular grid such as ours provides a reproducible initial condition and is consistent with previous work (Ferguson and Wathen, 1998).** ~~**so the tracers were most likely to move to natural positions from which further dispersion could be monitored.**~~

(6). The authors chose to organize the discussion of the results in three separate sections: 1) short presentation of a few sediment dispersion models in section 2.3, 2) test of these different models against the field data in section 3, 3) discussion in section 4. I don’t like this organization which prevents from conveying a clear message.

First of all, the reader loses track of the central idea of the manuscript. The accumulation of sentences starting with “We also ...” (at least 3 or 4 in sections 2.3.2 and 2.3.3) participates to this feeling and leaves the reader under the (false) impression that the authors are randomly testing theoretical models. Secondly, many notions are defined long before being actually used. E.g. the normalized transport distance defined page 1518 is plotted and discussed page 1524. Similarly, equation (2) or the dimensionless impulse are introduced page 1519 and used page 1525. Again, this does not facilitate the reading of the manuscript.

The authors should therefore reorganize the manuscript. It is particularly important to explain 1) what motivates the choice of a given model instead of another, 2) what are the differences between the different models (assumptions, physical mechanisms...).

We have reorganized several elements of the manuscript in response to these comments.

- *We revised subheadings in the methods and results so that the reader can easily track which methods lead to which results (e.g., where appropriate, we use the same subheads in each section) and eliminated some subheads.*
- *To more clearly convey the key elements of our analysis and to avoid the impression of randomly testing models, we eliminated one line of analysis (size-selective transport and comparison to Church and Hassan 1992), which we decided muddied, rather than clarified, our results. This resulted in elimination of sections of methods, results, and a figure.*
- *We attempted to more clearly explain choices of given models and differences among them.*
- *We attempted to define terms closer to where they were mentioned.*

See revised manuscript.

(7). page 1519, L1. D50 instead of L50

We have retained the original text; our scaled travel distance (using L50, as defined in the text) follows the convention of Milan (2013) and Church and Hassan (1992).

(8). page 1519, equation (2). I imagine that the coefficients involved in equation (2) (0.232, 1.35) are empirically fitted coefficients and not fundamental constants. If so, these coefficients probably depend on the field site where equation (2) is applied. The authors should comment on this.

Per our response to comment 6 above, we decided to eliminate the comparison of our results to the Church and Hassan (1992) size-selective transport equation (formerly Eq. 2). Some of the sites used in that equation were indeed quite different than our site.

(9). Page 1521. What motivates the choice of equations (5) and (6) to compute the critical Shields stress? To what extent do the values calculated from equations (5) and (6) differ from each other? From the empirical shields curve?

We selected these equations after literature review of approaches to calculating critical Shields stress in rivers that are comparable to our field site. We used the Mueller et al. approach (equation 5) because of the similarities between one of the streams from which their relation was developed (Halfmoon Creek) and the EFB in terms of morphology and hydroclimatic setting. To provide insight to the sensitivity of impulse to estimated critical Shields stress values, we chose to complement this with Recking's (2013; equation 6) approach, which is based on data from a large series of coarse-bedded rivers, including Halfmoon Creek, similar to Mueller et al (2005).

Differences in the Shields number are reflected in the I values (Table 4). Table 4 also has the Shields number approximations obtained using the equation – the Recking approach always provides larger*

Shields numbers than the Mueller approach. Our Shields number values correspond to the area of the Shields diagram where bedload transport would be expected.

Line 297

Because our tracer equipment could not directly detect initial motion~~the~~ conditions ~~under which particles were mobilized~~, we ~~instead~~ estimated ~~a range of~~ τ_c^* using two different empirical approaches,~~equations derived from similar~~ which we selected based on their derivation in gravel-bed systems similar to our study sites and our ability to measure required inputs. For the first estimate, we used Mueller et al.'s (2005) reference dimensionless shear stress relation for steep gravel and cobble-bed rivers:

$$\tau_{c,\mathrm{Mueller}}^* \approx \tau_r^* = 2.18S + 0.021 \quad (5)$$

where τ_r^* is a reference shear stress, which we assume is similar to τ_c^* (after Mueller et al., 2005). ~~The river in Mueller et al.'s study~~One of the study rivers in Mueller et al. (2005), Halfmoon Creek, is similar to our study site, as described above ~~with respect to channel dimensions, critical discharge, hydrology, elevation, and bed sediment characteristics~~. For the second estimate of τ_c^*, we used Recking's (2013) mobility shear stress (τ_m^*) equation, which was empirically developed using bedload transport data from gravel-bed transport studies in mountain~~ous~~ streams:

$$\tau_{c,Recking}^* \approx \tau_m^* = (5S + 0.06)\left(\frac{D_{84}}{D_{50}}\right)^{4.4\sqrt{S}-1.5}. \quad (6)$$

See revised manuscript.

(10). Many paragraphs address several different ideas and should therefore be split. See, for example, the very long paragraph of the introduction extending from page 1511, line 7 to page 1512, line 5. The paragraph starting p 1524, line 16 and ending page 1515, line 4 is another example.

We have edited the manuscript throughout in an effort to improve the writing, including spliting numerous paragraphs in the revised manuscript to better convey each idea separately and clearly.

(11). The phrasing of some sentences is rather unclear. I have listed some of them below. This list is not exhaustive and the authors might want to check the whole manuscript:

(a). page 1510, Line 18-19 : "We suggest that confluences absent of disturbances enhance sediment transport..."

(b). page 1513, Line 7-9 : "Sediment transport through equilibrium confluences, however, is poorly understood (Best and Rhoads, 2008), in turn constraining understanding of confluence influences on local and network-scale patterns of sediment routing."

(c). p. 1514, l. 21-22 "Between the study confluences is a plane-bed morphology control reach."

(d). p 1528, l. 6-7 "Despite this, observed tracer transport suggests that confluences enact an enhanced dispersive regime through increased travel distances and reduced depositional probabilities."

We have revised the phrasing of sentences in question (as well as other sentences throughout the manuscript) to improve clarity.

(12). Figure 3. The caption mentions “photographs of the (b) upper confluence, (c) control reach, and (d) lower confluence” which are not on the figure.

This was an error left over from a prior version of Figure 3 that included photos and has been corrected.

(13). Figure 5. Describe a, b, and c in caption.

Caption has been revised as suggested.

(14). The aspect ratio of figures 9, 10, and 11 should be increased so as to make them more readable.

Figures 9-10 have been revised as suggested, along with Figure 8.

(15). Figure 11. Modify axis limits to zoom in on the data.

Figure 11 has been removed from this manuscript, as described above.

Response to Reviewer #2 Comments
Kurt Imhoff
Andrew Wilcox

---

(1). Pg.2 ln.5-9 : This sentence is rather long. Perhaps consider something along the lines of "We investigate sediment routing patterns in headwater confluences by comparing them to low gradient gravel bed river reaches to characterize how confluences alter the transport of coarse clasts."

We have revised the sentence as follows:

Line 14

We investigated patterns and processes of sediment routing through headwater confluences by comparing them to published results from lower-gradient confluences and by comparing the dispersive behavior of coarse bedload particles between headwater confluence and non-confluence reaches.

(2). Pg.2 ln.16 : Tail analysis? I imagine you mean of the distribution of particle transport lengths, but at this point in the paper it is not clear what tail analysis means. Please add a couple of extra words of description.

We have revised the text as suggested:

Line 23

~~Stochastic transport modeling, tail analysis~~ Analysis of the distribution of particle transport lengths~~, and use of a dimensionless impulse (I*)~~ suggested that ~~transport distance and variance growth~~variation in the spatial distribution of coarse sediment particles ~~are~~ was ~~enhanced~~ enhanced by passing through confluences ~~for a given flow strength~~.

(3). Pg. 3 ln.9: This probably needs another citation earlier than Phillips et al (2013), I would suggest Einstein 1937 especially since the next three references directly build on his work. Phillips et al (2013) could be placed after Haschenburger (2013) in line 14.

We have revised the citations as suggested by incorporating Einstein (1937).

(4). I suggest added additional references here such as Nikora et al., (2002) and Metzler and Klafter (2000) which I think is a good introduction and review into diffusive processes from the physics literature.

We have revised the citations as suggested.

(5). You've already introduced PIT as the shorthand for passive-integrated transponder on pg 5 ln 16. It makes more sense to introduce it here where RFID is mentioned, so you could remove the earlier occurrence without any loss of clarity.

We have revised the text as suggested to avoid repeating ourselves.

(6). This line suggests that all of your particles are larger than the D50, suggest adding a percentage of particles greater than D50 or saying that most particles used were larger.

We have revised the description of the tracer particle sizes in response to comments by both reviewers; see response to Reviewer #1 comment 4.

(7). Figure 3 b, c, d seem to be missing. Adding them in would make the figure larger or require several figures but it would be conceptually useful to see the grain size distributions for reach tracer set with their field site bed grain size. If the control reach is slightly coarser that would support the hypothesis that confluences result in enhanced transport.

This was an error left over from a prior version of Figure 3 that included photos and has been corrected. Grain sizes are similar among study reaches (Table 2); we have therefore chosen not to plot the size distributions for each reach separately.

(8). Pg. 8 ln. 4: I don't think you need to keep reminding people of what PIT means.

We have revised the text as suggested.

(9). Pg. 8 ln. 4-14 : This paragraph could be omitted. It seems adequate to state the manufacturer, tag size, and the maximum read ranges and then refer to a citation where the reader if interested can find more information.

To address this comment we removed the bulk of the paragraph in question and reorganized section 2.2.

(10). Pg. 9 ln. 10-23: Please report the detection range of the loop antennae that you used and manufacturer if known.

We have added identification of the manufacturer where we first refer to the loop antenna. We have also added text clarifying how we determined the height above the bed at which our antenna should be deployed.

(11). Pg. 10 ln. 21 : Here <X/D> is the mean displacement length, which may not necessarily be the step length. Thinking about transport as steps and rests the step length represents (statistically) the average single displacement length from start to stop. A particle may move multiple times during a flood and thus, the resulting displacement length is a sum of an unknown (usually) number of steps.

We agree that "displacement length" is a more accurate term and have replaced "step length" with that here and in numerous other places in the manuscript.

(12). Pg. 11 ln. 20: Metzler and Klafter would be a good reference here. It is also important to consider that if your displacement data were heavy-tailed then rescaling it by the mean (<X/D>) wouldn't be correct because the longer you waited for the variance or mean of the data wouldn't converge. You might mention that you have tested the distributions to make sure that the mean is a meaningful parameter.

We agree, but look at it a bit differently. In testing whether the thin-tailed models applied to our data, we rescaled by the mean displacement and sought to determine whether it applied or not. Given the thin-tailed transport models we test, we considered the use of <X/D> to be appropriate.

(13). Pg. 12 ln. 1 : cumulative excess shear velocity rather than shear stress.

Text has been revised as suggested.

(14). Pg. 13 ln. 3: There are many rivers in Mueller et al. (2005), suggest rephrasing to say, Halfmoon creek, a river in Mueller et al. (2005) is similar to…

Text has been revised as suggested.

Line 306

~~The river in Mueller et al.'s study~~One of the study rivers in Mueller et al. (2005), Halfmoon Creek, is similar to our study site, as described above. ~~with respect to channel dimensions, critical discharge, hydrology, elevation, and bed sediment characteristics.~~

(15). Pg. 14 ln. 8-9 : It would help if you could describe what Parrett and Johnson (2004) is and then cite it rather than just referring to it without context.

Text has been revised as follows:

Line 159

We estimated the spring 2014 peak flow to have a 3.5 to 4-year recurrence interval, based on ~~used the~~ transducer data~~, along with Parrett and Johnson (2004) and analysis of a downstream US Geological Survey gauge, to estimate the peak discharge in 2014 as a 3.5 to 4 year event.~~, flood-frequency regression equations developed for western Montana streams (Parrett and Johnson, 2004), and analysis of a downstream US Geological Survey gage.

(16). Pg. 14 ln. 12 : Rather than list the average recovery percentage just give the range reported in table 2.

Text has been revised as follows:

Line 331

We recovered ~~of 75~~68–~~to~~ 86% of the seeded tracers, depending on the reach (Table 2).

(17). Figure 9. Dashed line should be labeled as exponential. It would help to add color or make the points larger in size, as it's hard to distinguish between Martin creek lower and upper. While the best fit exponential might not fit (in least-squares) the cloud of data well, the data seem to be straight enough on a semi-log plot that an exponential doesn't look bad at all for describing the overall trend (perhaps because I am having trouble discerning the trend for each reach with the current symbols). This plot does tell us that the data seem to collapse fairly well after normalizing by a single parameter (this provides quite a bit of support for a thin-tailed tracer displacement model, and even the exponential distribution which has a single parameter, except for that single point at far right). It doesn't look like there is any data below 10^-2, so maybe make that the lower bound and it'll be easier to see.

Some of the edits (labeled exponential, adjusted aspect ratio) are straightforward and we agree with their implementation.

It is certainly possible that the thin-tailed model is appropriate here. We note in the manuscript that the models fit the data reasonably well (except for the tails), and that power-law fits in Figure 10 suggest that the tracer data lies around the thin-heavy tail threshold. We have revised the text in an effort to more clearly make the points that (1) the control reach is thinner-tailed, and (2) confluences enact generally heavier-tailed distributions of particle transport relative to the control reach, but the enhanced dispersive effects could take place entirely within a thin or heavy-tailed regime as long as confluence particles are traveling further on average and experiencing heavier tails.

See revised manuscript (discussion)

(18). Figure 10. It's not clear to me why starting the tail at 80% (8*10^-1) is correct. Given that each distribution has a substantial break in slope after this point, in the case of the lower martin creek it is close to the 20% mark. In terms of exceedance probability the first 10-20% is the left tail (low transport distances) and 20-80% is the middle of the distribution. Still some of the data may have lower slope than -2 (for reference it would help if a -2 slope were added to the plot), but only barely. This interpretation also seems to conflict with figure 9 in which the data seems to be relatively straight on a semi-log plot, which does not support a heavy-tailed power law distribution. It would also help to have the power-law fits to the tail region where you determine which ones are heavy-tailed or not. This could be done in the same way that Hassan et al. (2013) do their analysis. Something should also be mentioned about how tracer recovery percentage affects the scaling of the tail parameter (see Hassan et al., 2013). If you decide to assess the tail parameter, though, please describe the method that was used. At the moment it is not clear if the data were fit by a power law or a more rigorous approach like the Hill estimator was used.

*We think there is some confusion as to what is meant by 80%. We refer to the 80th percentile of tracer transport distances, not the value of 8*10^-1 on the y-axis. We simply tested various slope break locations in the vicinity of 80% and determined that for this analysis, the results (thin vs. heavy tail) were not sensitive to where we started the tail.*

As stated earlier, we don't wish to assert that all confluences are heavy-tailed, but rather that in the case of the EFB they are "heavier" than the control reach, indicating a larger proportion of tracers traveling relatively far distances. We consider this important in itself, regardless of whether they all fell within the "thin" or "heavy" tailed distinction – the confluences seem to be associated with heavier tails, in which a greater proportion of tracers travel relatively far distances compared to the mean.

We found amending Figure 10 to show the tail extent, power-law equation, and slope of the exceedance tail to clutter up the figure. We went with an approach that shows the alpha (slope) of the decay next to each creek in the legend. We hope that this, combined with written edits to make clear that we are following Hassan et al. (2013)'s convention, are a satisfactory edit.

See revised manuscript.

(19). Figure 11. Other figures would benefit from a similar color and symbol scheme as used in this figure.

Figures 9 – 10 have been revised to add color and use a similar symbol scheme as Figure 11, though Figure 11 has now been removed – as we decided it muddied, rather than clarified, our results. This resulted in elimination of sections of methods, results, and a figure.

See revised manuscript

(20). Figure 12. Could you label which reaches the points are from? In the text (pg17 ln24) it states that the variance follows a power-law relation, but it seems that a linear line is plotted. Unless the exponent was left off of the equation given. Could you comment on why the relationship for the different populations of tracer particles should fall on the same linear line or why they are related linearly? In phillips and jerolmack (2014) tracer particles for their two field sites fell on two different linear relationships and in order to fit them onto a single curve the frictional resistance of the stream bed needed to be accounted for. Does normalizing I* by frictional resistance provide a better collapse of the data?

Labeling the reaches all on the plot makes the figure much more difficult to interpret. We revisited the figure, and have added the correct linear and power-law equations to the figure – there had been a mistake, with an incorrect set of equations shown in the original Figure 12 – we are grateful to have revisited it.

Normalizing did not significantly affect the collapse of our data, but we have mentioned it in Section 3.3.Section 3.3 also has reference to why the linear relationship occurs and what it means.

(21). Pg. 17 ln. 25 : the linear relationship in Lajeunesse et al. (2010) is for average step length against shields stress for constant flow, whereas the results given and those of Phillips and colleagues are for total displacement in unsteady flow. These are likely related, but it has not been shown nor is it obvious to me how they are related. Perhaps leave the Lajeunesse citation out of this line.

We have deleted the Lajeunesse et al. citation here, as suggested.

(22). Pg. 18 ln. 12-15 : It is not clear if these lines are suggesting that upstream geometry and bed discordance are minimal for morphodynamics in general or just for this river (because they are simple and minimal).

We have revised the text to clarify that upstream geometry and bed discordance are important variables in general but not at our sites:

Line 435

…reflect the controlling influences of θ and Q_r; the simple upstream planform geometry and minimal bed discordance at our sites suggest that these factors ~~have less~~exert little influence on ~~confluence~~ morphodynamics in our study confluences.

(23). Pg. 20 ln. 9-12 and parts of the conclusion: If confluences enhance coarse particle transport more than the standard plane bed reach then shouldn't there be enhanced deposition between the upper and lower confluences or is the conceptual model hypothesizing that coarse particle transport continues to increase with additional equilibrium confluences? Did you observe enhanced deposition or a coarser bed between the upper and lower confluence sites? The conclusions suggest that the interpretation of the confluences is that they locally enhance transport of coarse material, so in order for mass to balance there should be a noticeably (if the effect is strong) coarser bed between the confluences. If you have the particle size data, it would be interesting to look at this.

The comment is insightful, although we do not have the data to evaluate morphodynamic linkages in a mass balance framework. We have revised the last sentence of the conclusion to suggest that linking tracer studies with measurement of bed texture and elevation would further clarify the issues we examined here. We have also revised other elements of the discussion and conclusion in the context of our responses to reviewer comments to clarify our key points.

See revised manuscript

(24). It is nice to see the tracer displacement data published with the paper and in general, the supplementary data and explanations are well done. Figure S5 should probably be shown with straight lines rather than curved lines. I encourage the authors to upload their tracer data to a digital repository as well (Figshare comes to mind because it is free and provides a citable DOI).

We have uploaded our data to a repository, but it was incorrectly displayed in the original link. It has now been fixed, and the tracer pre and post-flood locations can be accessed.

Coarse bedload routing and dispersion through tributary confluences

Kurt S. Imhoff[1*], Andrew C. Wilcox[1]

[1] Department of Geosciences, 32 Campus Drive #1296, University of Montana, Missoula, MT 59812

Correspondence to: kurt.imhoff@umontana.edu

Abstract

Sediment routing fundamentally influences channel morphology and propagation of disturbances such as debris flows. ~~However, t~~The transport and storage of bedload particles ~~in~~ across headwater channel confluences, which may be significant nodes of the channel network in terms of sediment routing, morphology, and habitat, ~~is~~ are poorly understood, however. ~~To characterize~~We investigated patterns and processes of sediment routing ~~patterns processes~~ through ~~confluences of headwater channels, we investigate how sediment routing patterns through headwater confluences compare~~headwater confluences by comparing them to published results from~~patterns observed to those described in~~ lower-gradient ~~gravel-bed river systems,~~confluences and by comparing the~~. D~~ dispersive behavior of ~~and how confluences affect the dispersive behavior of~~ coarse bedload particles ~~is also compared to~~ between headwater confluence and non-confluence reaches. We addressed these questions with a field tracer experiment using passive-integrated transponder and radio-frequency identification technology in the East Fork Bitterroot River basin, Montana, USA. Within the confluence zone, transport ~~occurs~~ occurred along scour-hole margins in narrow, efficient transport corridors that mirror those observed in ~~finer-grained~~prior ~~experiments and field~~ studies, many of which ~~occur in~~are from finer-grained systems. Coarse particles entering confluences experience reduced depositional probabilities, in contrast to the size-selective transport observed in a control reach. ~~Stochastic transport modeling, tail analysis, a~~Analysis of the distribution of particle transport lengths~~, and use of a dimensionless impulse (I*)~~ suggested that ~~transport distance and variance growth~~variation in the spatial distribution of coarse sediment particles ~~are~~ is enhanced by passing

through confluences~~ for a given flow strength~~. We suggest that equilibrium confluences ~~absent of disturbances~~ can enhance sediment transport ~~and dispersive growth~~ through headwater networks.

1 Introduction

The ~~spatiotemporal~~ transport and storage ~~patterns~~ of mobile sediment particles through channel networks, i.e., sediment routing (Swanson and Fredriksen, 1982), ~~governs channel evolution in alluvial rivers by~~ link~~ing~~ sediment supply, flow, and channel morphology and thereby regulate channel evolution (Church, 2002; Church 2006). In headwater regions, where hillslope-channel connectivity is strong, storage and downstream routing of sediment inputs reflect the influence of ~~and streams are sensitive to~~ spatially and temporally variable forcing by hillslope (e.g., debris flows) and fluvial processes ~~and land-use change~~ (Montgomery and Buffington, 1997; Brooks and Brierley, 1997; Prosser et al., 2001;~~), debris flows or fluvial processes result in storage and downstream routing of sediment inputs (~~ Lancaster and Casebeer, 2007). Discrete pulses of coarse sediment delivered to streams can travel downstream as a translating bedload wave, by dispersion~~as a dispersive process~~, or by~~as some~~ a combination of translation and dispersion (Lisle et al., 2001; Sklar et al., 2009).

Analyses of dispersion based on the premise that particle motion is a random walk have represented downstream transport as a series of intermittent steps and rests (~~Phillips et al., 2013~~Einstein, 1937). This approach has informed flume and field studies seeking to identify characteristic probability distributions of step length and rest periods (e.g., Hubbell and Sayre, 1964; Yang and Sayre, 1971; Bradley et al., 2010). Statistical distributions, including exponential, gamma, and Pareto functions, have been found to approximate spatial distributions of bedload~~-~~particle displacements in flume and field conditions (e.g., Hassan et al., 1991; Bradley and Tucker, 2012; Martin et al., 2012; Haschenburger, 2013, Phillips et al., 2013). These statistical models have been used to approximate dispersive regimes in various gravel-bed channel morphologies, includ~~explor~~ing plane-bed (Bradley and Tucker, 2012), pool-riffle

(Liébault et al., 2012; Milan, 2013), and braided systems (Kasprak et al., 2014). Many model functions may be applicable, however, because morphologic features and hydraulics can produce characteristic local dispersive regimes (Pyrce and Ashmore, 2003). Long-term tracer experiments have noted evolving spatial distributions of bedload particles, suggesting that best-fit statistical distributions may differ depending on the degree of vertical mixing, often a function of time (Haschenburger, 2013). As a result, dispersion models predicting a smooth spatial distribution may not adequately capture the true dispersive behavior of bedload particles across multiple channel morphologies.

~~More recent study of coarse bedload transport has considered t~~The dispersive behavior of coarse sediment particles has also been considered in terms of changes in the variance of particle displacements with time (e.g., Phillips et al., 2013). Sediment dispersion is thus treated as analogous to one-dimensional diffusion in the downstream direction, with potential diffusion dynamics that include normal diffusion, where the variance of particle displacements increases linearly with time, and anomalous diffusion, which includes both superdiffusion and subdiffusion, when variance increases more quickly or more slowly with time than the linear case, respectively (Metzler and Klafter, 2000; Nikora et al., 2002; Olinde and Johnson, 2015). ~~Predictions of sediment routing require an~~ I~~i~~mproved understanding of variability in dispersive regimes among channel types and other controls on sediment dispersion is needed, however, to facilitate sediment-routing predictions.

Nodes of the channel network that may be especially important with respect to sediment routing are tributary confluences, where point ~~-~~sources of flow and sediment connect tributary to trunk streams. The importance of confluences in sediment routing, as well as their morphologic significance, may depend on factors including ~~stream~~ drainage densities (i.e., frequency of confluences) (Benda et al., 2004), the magnitude and frequency of disturbances such as debris flows (Benda and Dunne, 1997; Hoffman and Gabet, 2007), and the relative differences in flow, sediment caliber, and load between tributaries and the trunk streams they enter (Figure 1) (Knighton, 1980; Richards, 1980, Ferguson et al., 2006, Swanson and Meyer, 2014). ~~The m~~Morphological effects stemming from disturbance-derived confluence deposits may extend spatially, well beyond the area of flow convergence, and temporally, persisting for ~10^2 – 10^4

years (Lancaster and Casebeer, 2007). Study of confluences in light of disturbance deposits and morphological heterogeneity has led to the Network Variance Model (NVM, Benda et al., 2004), which considers the spatial arrangement of confluences in river networks and how they affect local and non-local channel morphological characteristics. Channel confluences also represent biological "hot spots", forcing spatial heterogeneity in habitat types and in various habitat metrics and influencing longitudinal distributions of aquatic organisms (Rice et al., 2001; Gomi et al., 2002).

Whereas sediment dynamics and morphology of headwater confluences can be primarily influenced by disturbances such as debris flows (Benda and Dunne, 1997), what we refer to as "equilibrium" confluence morphology, reflecting feedbacks between flow hydraulics, sediment transport, and morphology, can also develop and persist (Figure 1). Such confluences~~, which~~ are well-studied in sand and gravel-bed river systems ~~(e.g., Best, 1987; Rhoads, 1987; Roy and Bergeron, 1990; Biron et al., 1996; Boyer, 2006; Rhoads et al., 2009),~~ and typically feature a central scour hole, tributary-mouth bars, and bank-attached bars at areas of flow recirculation and stagnation (~~(e.g.,~~ Best, 1987; Rhoads, 1987;~~ Roy and Bergeron, 1990; Biron et al., 1996; Boyer, 2006; Rhoads et al., 2009),~~Best, 1988; Roy and Bergeron, 1990; Biron et al., 1996; Boyer, 2006; Rhoads et al., 2009; Ribeiro et al., 2012). ~~Hydraulics responsible for the formation of this morphology relate to p~~Physical controls on confluence hydraulics and associated morphology include~~ing~~ junction angle (ϴ), bed discordance (z_d), discharge ratio (Q_r) (Figure 1), and upstream planform curvature (Ashmore and Parker, 1983; Best, 1987; Biron et al., 1996; Rhoads and Sukholodov, 2004; Boyer et al., 2006; Constantinescu et al., 2012; Ribeiro et al., 2012). Sediment transport through equilibrium confluences, however, is poorly understood (Best and Rhoads, 2008),~~.,~~ ~~in turn constraining~~limiting understanding of how confluences influence~~s~~ ~~on~~ local and network-scale patterns of sediment routing.

In this study we assess how coarse bedload particles are routed through equilibrium confluences in a mountain river headwaters. We address two questions: i) How do sediment routing patterns through headwater confluences compare to those described in other, primarily lower-gradient gravel-bed river systems? ii) How do confluences affect the dispersive behavior of coarse bedload particles compared to non-confluence reaches? We address these questions with a tracer experiment ~~, using passive-integrated transponder (PIT) tags,~~ conducted through two headwater confluences and a non-confluence control reach. We ~~employ~~ compare established sediment transport models ~~, tracer analyses,~~ and a dimensionless impulse framework (Phillips et al., 2013) to observed tracer behavior to explore the effects of confluences on sediment transport and dispersi~~ve behavior~~on. ~~Lastly, we compare~~We also evaluate our results and their implications in the context of~~with~~ theory regarding confluences and sediment routing through headwater networks. Our study contributes to the growing body of work on particle dispersion and transport dynamics in mountain rivers and is, to our knowledge, the first to investigate these topics with respect to sediment routing through confluences in a field setting.

2 Methods

Here we describe our study area and the preparation, deployment, and measurement of coarse-bedload tracer particles. We then describe the analyses we conducted that allow comparison of particle displacement through the study confluences to that of the control reach and prior transport studies in gravel-bed river systems. This involved assessment of displacement distributions and a dimensionless impulse, with the goal of evaluating and comparing dispersive regimes. Additional details on these analyses, beyond what is provided below, are in Supplemental Information and Imhoff (2015).

2.1 Study area

We selected a study area in the East Fork Bitterroot (EFB) River basin in western Montana, USA (Figure 2) that is typical of semiarid, snowmelt-dominated, montane headwater systems. This location lacks recent physical disturbances (e.g., post-wildfire debris flows) and contains confluences exhibiting characteristics of the equilibrium morphology described above. The field site drains 298 km^2 of forested and alpine mountainous terrain, in both the Sapphire Mountains and Pintler Range, ranging in elevation from 1584 m to 2895 m. Sediment supplied to channels is comprised of quartzite, argillite, siltite, and feldspathic granitic rock, eroded from metasedimentary Belt Supergroup and Idaho Batholith sources. Annual precipitation is about 0.6 m yr^{-1}, based on data from the Tepee Point weather station 1.4 km from the EFB (Western

Regional Climate Center Remote Automated Weather Station, 2015). Runoff is dominated by spring snowmelt, with flows capable of mobilizing coarse bedload typically occurring in similar streams between March and July. Human influences from roads and other land uses are minimal in the study area.

Two tributary confluences mark the upstream and downstream extent of the study area. These are herein referred to as the upper confluence, where Moose Creek and Martin Creek combine, and, 1 km downstream, the lower confluence, where Martin Creek enters the EFB. The tributary and mainstem stream of each study confluence are considered as separate reaches, for the purpose of separately considering incipient motion and transport behavior of tracers starting in each. Between the study confluences is a plane-bed ~~morphology~~ control reach. Combined discharge in the upper confluence is approximately half that of the lower confluence.

~~Depositional bars are present behind large flow obstructions such as logs or large boulders, and along channel margins.~~ Because the site is ungauged, we installed HOBO-U20 water level loggers to record stage at 15-minute intervals during the 2014 study period. One transducer was placed along a surveyed-cross section of the bed at each study reach. We also periodically manually measured water surface elevations and, during wadeable conditions, stream velocities. Above-average flows during the study period reflected that year's large snowpack. Snow water equivalent at SNOTEL sites within 50 km of the study area registered above 150% of normal on 1 April 2014 (http://www.wcc.nrcs.usda.gov/snow/). We estimated the spring 2014 peak flow to have ~~corresponding flood as~~ a 3.5 to 4-year recurrence interval, ~~event~~ based on transducer data, flood-frequency regression equations developed for western Montana streams (Parrett and Johnson, 2004), and analysis of a downstream US Geological Survey gage. Flood flows peaked between 25 May ~~25~~ and 4 June ~~4,~~ 2014 (Figure 3).

To characterize study-reach morphology, we completed topographic surveys and grain-size measurements. Topography was surveyed using a Leica TS06 total station during the initial tracer deployment (March 2014), before spring runoff high flows, and the summer (July-September) recovery campaign. Topographic surveys entailed longitudinal profiles, to determine slope, and cross-sections at the location of pressure transducers, for use in the incipient motion estimates described below. We also surveyed bedform extents to produce a bedform map. Surface grain size distributions were measured using Wolman pebble counts across each study reach. Channel slopes, dimensions, grain sizes, and confluence characteristics are shown in Table 1 (also see Supplemental Information).

2.2 ~~Tracer preparation, deployment, and measurement~~Bedload tracer preparation, deployment, and measurement

Our study employed passive-integrated transponder (PIT) and radio-frequency identification (RFID) technology for tagging and tracing bedload particles. PIT tags are highly recoverable, durable, and cost-effective relative to other particle tracing methods (e.g., Lamarre et al., 2005; Bradley and Tucker, 2012; Chapuis et al., 2015). Moreover, PIT-tagging allows for analyses of transport of both bed-material populations and specific subsets of the grain population (e.g., by size, shape, lithology), ~~step-length~~displacement distributions and their evolution over time, and other aspects of transport dynamics.

We collected gravel and cobble particles from Moose Creek, upstream of our study reaches, in January 2014 for tagging. Using a 1-hp drill press, holes 8 mm wide by 30 mm long were drilled using a ~0.8 mm diamond-tipped drill bit.~~ Tracer particles used were generally larger than the bed D_{50} (Table 1), as particles with b-axis axes below 45 mm often fractured during drilling.~~ We tagged cobbles with median axes mostly between 60 and 130 mm (Figure ~~3~~4, Table 2). Many of the tracer particles were larger than the bed D_{50} (Table 1), because particles with b-axes below 45 mm often fractured during drilling. ~~This represents the D_{37} to D_{70} size fraction, which we~~ We assumed our tracer particles, which fell within the D_{37} to D_{70} size fraction of bed materials, to be representative of the coarser fraction of mobile ~~bedload particles~~bedload particles. ~~The D_{50} of our tagged tracers varied between 0.077 m and 0.082 m (Table 2).~~The results and interpretation of our sediment tracers thus do not apply for the entire mobile bedload population in this system.

The ~~passive-integrated transponder~~ ~~(~~PIT~~)~~ tags used in this study are 12 mm and 23 mm half-duplex, read-only tags from Oregon RFID. Vertical read range varies based on tag orientation, battery level, noise proximity, and other factors, but is generally 0.25 to 0.5 m. Previous work has identified horizontal and vertical detection ranges at 0.5 m (Lamarre et al., 2005) and 0.25 m (Bradley and Tucker, 2012)~~-~~. Chapuis et al. (2014) assessed RFID detection ranges ~~in depth,~~ and observed higher uncertainty in radial detection distance than reported in other studies. ~~The most u~~Uncertainty in tracer position is highest for ~~that of a~~ solitary, buried tracers, which are~~is~~ not visible via snorkel survey and have~~s~~ the largest detection radius;~~—~~ clusters of buried tracers, in contrast, have reduced detection ranges via tag interference. We oriented the antenna parallel to the surface of the bed, at a height of about 0.2 m (after Chapuis et al., 2014). For our analysis, we considered tracer movement below the threshold of detection as immobile and assigned a travel distance of 0 m (~~,~~after Phillips and Jerolmack, ~~(~~2014). Particles moving beyond the threshold of detection were labeled the “mobile” fraction. In total, 428 cobble and gravel tracers were prepared for deposition into the three study reaches (~~; these were distributed among sites as shown in~~ Table 2).~~Each tag is comprised of a glass-encapsulated pulse transponder that emits a unique identification code when activated (Lamarre et al., 2008). By deploying a reading unit and control unit, an electromagnetic signal can be emitted that briefly powers the passive transponder, which then transmits its unique identification code. Inserted PIT tags were sealed in tracer particles with marine epoxy. The tags were activated and the identity and size of each rock recorded prior to deployment. Liébault et al., (2012) found post-drilling density differences to be small (3–5%), so we did not consider the density differences post-implantation in this study. In total, 428 cobble and gravel tracers were prepared for deposition into the three study reaches; these were distributed among sites as shown in Table 2.~~

We installed the PIT-tagged tracers before the onset of the spring snowmelt, in late March and early April 2014. Our seeding method ~~emulated that employed by Ferguson and Wathen (1998): particles were seeded loosely~~involved loosely seeding tracer particles on the bed surface near the channel thalweg in a ~~random~~ grid (Figure 5). Mimicking the arrangement of fluvially-deposited gravels and minimizing the influence of the initial condition of particle deployment is a challenge in tracer studies, but a regular grid such as ours ~~at least~~ provides a reproducible initial condition and is consistent with previous work (Ferguson and Wathen, 1998).~~, an established and easily reproducible initial condition for coarse particle tracer studies. so the tracers were most likely to move to natural positions from which further dispersion could be monitored. Additionally, a~~A sparse grid like the one employed here ~~helps avoid~~minimizes disturbance to the bed and flow field (Bradley and Tucker, 2012) while simultaneously avoiding “confusing” the PIT tag detection equipment, which encounters issues when dealing with clusters of particles (Chapuis et al., 2014). The gridded surface ranged from 7–13 m wide. We deployed PIT-tagged tracers at equal distances upstream from the confluence in each tributary. Initial tracer positions were recorded using the total station.

Field recovery campaigns to detect tracer locations and measure particle displacement took place after recession of high flows, once the streams were wadeable. ~~This entailed scanning the bed~~The bed was scanned with a 0.5 m diameter loop antenna~~,~~ in conjunction with a backpack reader. Once a tracer was located, the loop antenna was brought towards its detection field from all directions. This helped to identify other tracers in a cluster by reading different tags first, depending on the direction the cluster is approached. Each tracer’s position was recorded using the total station. The uncertainty associated with individual total station ~~introduces error in~~ measurements of tracer position and travel distance is ±~~. Individual measurements for the Leica total station have an inherent uncertainty of ±~~ 0.20 m. We also employed a snorkel survey to identify if tracers were ~~exposed on the bed~~buried or clustered together. Visible tracers were occasionally surrounded by other tracers in shallow pockets. At all sites, we scanned with the loop antenna for 200 m downstream of the last detected particle to limit omission of any far-traveling tracers, which influence the tail character of ~~step-length~~displacement distributions. The position of far-traveling tracers was recorded with a Trimble GEOXH 6000 GPS.

~~Both the total station and loop antenna introduce error in measurements of tracer position and travel distance. Individual measurements for the Leica total station have an inherent uncertainty of ± 0.20 m. The detection range for the loop antenna differs based on the orientation of the PIT tag relative to that of the loLamarre et al. (2005) identified horizontal and vertical detection ranges at 0.35 and 0.5 m, respectively, and Bradley and Tucker (2012) record a vertical range of 0.25 m. An in-depth assessment of RFID detection ranges is presented by Chapuis et al. (2014), and identifies higher uncertainty in radial detection distance than reported in other studies. The most uncertain tracer position is that of a solitary, buried tracer, which is not visible via snorkel survey and has the largest detection radius – clusters of buried tracers have reduced detection ranges via tag interference. We oriented the antenna parallel to the surface of the bed, at a height of about 0.2 m (after Chapuis et al., 2014), which corresponded to the distance we typically~~

~~detected PIT tags in pre-field experiments. For our analysis, we considered tracers moving greater than 0.2 m as the "mobile" fraction; tracers measured as moving 0.2 m or less were considered immobile and assigned a travel distance of 0 m.~~

~~2.3 Transport analyses~~

~~We conducted a suite of analyses to evaluate how particle displacement through the study confluences compared to that of the control reach.~~ ~~We assessed stochastic sediment transport models of sediment dispersion across our study site, scaled tracer transport and tail character, and a dimensionless impulse, with the goal of evaluating and comparing dispersive regimes. Additional details on these analyses, beyond what is provided below, are in Supplemental Information and Imhoff (2015).~~

2.3~~.1 Stochastic sediment transport modelling~~Particle displacement distributions

To ~~characterize~~evaluate observed particle displacement distributions ~~population transport dynamics~~ across our study site,~~To determine whether step-length distributions in confluence reaches differ from those in the control reach,~~ we tested the applicability of two stochastic models of sediment transport and dispersion: the Einstein-Hubbell-Sayre (EHS; Hubbell and Sayre, 1964) and Gamma-Exponential models (GEM; Yang and Sayre, 1971). These models were chosen following previous tracer experiments, particularly Bradley and Tucker (2012), who tested the fit of ~~because~~ the EHS and GEM functions ~~have been used~~ to ~~fit~~ step-length probability distributions measured using PIT tags in Halfmoon Creek, Colorado, USA. Halfmoon Creek has similarities in terms of slope, grain size, width, plane-bed morphology, and snowmelt hydrology to our study sites and is thus suitable for comparison with our results~~for a similar plane-bed reach in Colorado (Halfmoon Creek; Bradley and Tucker, 2012); our tracer seeding methods were similar to that study~~. ~~This recent application of the EHS and GEM functions in similar systems led us to apply them towards our study confluences as a form of comparison.~~ The ~~primary difference between the~~ EHS and GEM models ~~is~~ differ by modeling step lengths using either ~~whether or not the distribution of step lengths monotonically decreases (EHS) or not (GEM), through the use of~~ exponential (EHS) or~~and~~ gamma (GEM) distributions, resulting in step-length distributions that decrease monotonically (EHS) or vary more flexibly (GEM), as described in more detail in ~~for step length, respectively. Comprehensive background on the use of these models is provided by~~ Bradley and Tucker (2012) and in our Supplemental Information. We compared EHS and GEM fits to our confluence and non-confluence transport data, with the goal of comparing bulk routing characteristics between the two reach types. In doing so we ~~assume that these~~apply models that~~, which~~ approximate step length~~, are adequate~~ to test against observed displacement, which for an individual particle may ~~likely~~ include multiple steps across the 2014 hydrographs~~ a different number of step lengths for different particles~~.

~~**2.3.2 Modal transport and tail analysis**~~

~~The EHS and GEM involve thin-tailed distributions of step length, which we assume to apply to displacement over the course of the 2014 flood. o determine~~To further investigate displacement distributions, we assessed dimensionless transport distances of each tracer~~, i.e., modal transport distance,~~ ~~we scaled~~by scaling each tracer's transport distance (X_i) by its median diameter (D_i). We then calculated normalized transport distance, X_n (after Phillips et al., 2013):

$$X_n = \frac{\frac{X_i}{D_i}}{\langle \frac{X}{D} \rangle} \qquad (1)$$

where (<X/D>) is the mean ~~step~~ displacement length for the 2014 flood at each study reach. In addition~~Relative tracer transport distances and group statistics can thus be compared among populations of mobile particles.~~

~~Thirdly~~, we analyzed cumulative exceedance distributions of tracer travel distance for each study reach to assess tail character (~~,~~after Hassan et al.~~,~~ ~~(~~2013). This was achieved by measuring the rate of decay of the exceedance distribution tail, $P(X>x)$, where X is a travel distance beyond the user-determined start of the tail, x. The log-log slope of decay (α) distinguishes between~~, and~~ heavy-tailed ($\alpha < 2$) and thin-tailed ~~-~~($\alpha>2$) distributions ~~tailedness is defined as when the log-log slope of decay (α) is less than 2~~ (after Hassan et al., 2013)~~.~~ ~~The mean and variance of step-length distributions converge to finite values in thin-tailed cases ($\alpha>2$); the mean is finite but variance non-convergent when $1< \alpha<2$; neither mean nor variance converge to finite values when $\alpha<1$~~ (Metzler and Klafter, 2000; Olinde and Johnson, 2015). We considered <X/D> to be a suitable parameter to test in the context of comparing our tracer data to thin-tailed transport models.

These analyses offer a comprehensive approach to investigating whether the overall distribution of particles evolves in a significantly different way when being routed through confluences, as opposed to the plane-bed control reach.

~~We also investigated size-selective transport by plotting scaled travel distance ($L^* = L_i/L_{50}$) against scaled tracer size ($D^* = D_x/D_{50}$) for 10 mm subsets of our tracers, where L_i is the mean travel distance of each subset, L_{50} the mean travel distance for the entire population, D_x the mean value of each subset, and D_{50} the median grain size of the bed. We also assessedassessed how our transport distance-grain size relationship compared to the empirical, size-dependent transport relationship for gravel-bed rivers developed by Church and Hassan (1992) from a compilation of painted-rock studies:~~

$$\cancel{\log L^* = 0.232 + 1.35\log(1 - \log D^*),} \qquad \cancel{(2)}$$

~~a relationship that suggests that, as scaled particle size increases, scaled travel distance decreases. While the coefficients in Eq. 2 used here are empirically fittedstreams with a range of bed textures and hydrologic regimes (, we note the similarity between the EFB and many of the streams investigated by Church and Hassan, (1992), and assume the basic relationship observed betweenuse Eq. 2 to assess the basic relationship between size and travel distance for our particle tracers. particle size and travel distances should apply at the EFB.~~

~~A second method for assessing the evolution of sediment pulses in right-skewed statistical distributions is to analyze tail character of a tracer population (Hassan et al., 2013). Heavy-tailed step-length distributions occur when a large proportion of particles travel relatively long distances. We analyzed cumulative exceedance distributions of tracer travel distance for each study reach to assess tail character. This was achieved by measuring the rate of decay of the exceedance distribution tail, P(X>x), where X is a travel distance beyond the user-determined start of the tail, x, and heavy tailedness is defined as when the log-log slope of decay (α) is less than 2 (after Hassan et al., 2013). The mean and variance of step-length distributions converge to finite values in thin-tailed cases (α>2); the mean is finite but variance non-convergent when 1< α<2; neither mean nor variance converge to finite values when α<1 (Metzler and Klafter, 2000;~~

~~Olinde and Johnson, 2015). We assumed <X/D> to be a meaningful parameter to test, given our comparison of our tracer data to thin-tailed transport models.~~

2.3.~~3~~ 2 ~~Incipient motion and dimensionless impulse~~Dimensionless impulse

We also analyzed tracer data~~Our tracer data awere analyzed~~ with respect to a cumulative dimensionless impulse~~,~~ I*, that links particle displacement to the duration of flow above the threshold of motion (~~Equation 3~~Phillips et al., 2013)~~, determined for each of our five seed reaches. I* allows for a fluid momentum conservation approach to analyze long-term tracer displacement data and was developed to allow for pairing such data with simple flow and bed measurements. We used I* to compare tracer transport distances against the cumulative excess shear velocitystress imparted on grains. When comparing confluence and non-confluence reaches, we considered deviation from a linear relationship between <X/D> and I* (Phillips et al., 2013) to constitute a difference in dispersive regimes. The impulse, I*, is defined~~ as follows:

$$I^* = \int_{t_i}^{t_f} \frac{(U_e^*)dt}{D_{50}} \qquad (~~3~~2)$$

where t_i and t_f are start and end times, respectively, for flow above a critical threshold of motion of bed materials, and U^*_e is excess shear velocity, which is the difference between the shear velocity (U^*) and the critical shear velocity (U_c^*) associated with initial motion of bed particles. Flume studies have identified that a mobilized sediment particle shows a ~~step length~~ total displacement that is proportional to U^*_e (Lajeunesse et al., 2010; Martin et al., 2012). Shear velocity is equal to $(gRS)^{0.5}$~~.~~, where g is gravitational acceleration, R is hydraulic radius, and S is channel slope. ~~; f~~For the critical condition (U_c^*), R_c is critical hydraulic radius associated with the mobilization of the average-sized tracer particle and can be~~. We~~ back-calculated ~~R_c~~ from critical Shields number (τ_c^*), a non-dimensional shear stress associated with incipient motion of particles in a flow:

$$\tau_c^* = \frac{\rho g R_c S}{(\rho_s - \rho_w) g D_{50}} \qquad (~~4~~3)$$

where ρ_s is sediment bulk density (assumed to equal 2650 kg m^{-3}) and ρ_w is water density (1000 kg m^{-3}).

We used I* to compare tracer transport distances against the cumulative excess shear velocity imparted on grains. We determined I* for each of our five seed reaches and, as a means of comparing confluence and non-confluence reaches, evaluated the extent to which each data set deviated from a linear relationship between <X/D> and I*, which can be considered indicative of a difference in dispersive regimes (Phillips et al., 2013).

Because our tracer equipment could not directly detect initial motion~~the~~ conditions~~ under which particles were mobilized~~, we ~~instead ~~estimated ~~a range of ~~τ_c^* using two different empirical ~~equations ~~approaches, which we selected based on their derivation~~ derived~~ ~~from ~~in ~~similar~~ gravel-bed systems similar to our study sites and our ability to measure required inputs. For the first estimate, we used Mueller et al.'s (2005) reference dimensionless shear stress relation for steep gravel and cobble-bed rivers:

$$\tau^*_{c,\mathrm{Mueller}} \approx \tau^*_r = 2.18S + 0.021 \qquad (\cancel{5}4)$$

where τ_r^* is a reference shear stress, which we assume is similar to τ_c^* (after Mueller et al., 2005). ~~The river in Mueller et al.'s study, Halfmoon Creek,~~~~Halfmoon Creek, ~~O~~o~~ne of the study rivers in Mueller et al. (2005), Halfmoon Creek, is similar to our study site, as described above ~~with respect to channel dimensions, critical discharge, hydrology, elevation, and bed sediment characteristics~~. For a second estimate of τ_c^*, we used Recking's (2013) mobility shear stress (τ_m^*) equation, which was empirically developed using bedload transport data from gravel-bed transport studies in mountain~~ous~~ streams:

$$\tau^*_{c,Recking} \approx \tau^*_m = (5S + 0.06)\left(\frac{D_{84}}{D_{50}}\right)^{4.4\sqrt{S}-1.5}. \qquad (\cancel{6}5)$$

~~where D_{84} is the 84th percentile grain size. ~~Analogously to~~s with~~ Eq. (5), we assume τ_m^* approximates τ_c^* (after Recking, 2013).~~ Both estimates were chosen due to their use of many gravel-bed systems similar to the EFB, as well as the relatively few inputs required to calculate~~

~~Shields stress. This rendered the Mueller and Recking approaches as ideal for our field study of coarse sediment tracers. Ranges of τ_c^* are produced by these two approaches are reasonable and shown in Table 4.~~

These two estimates for τ_c^* were paired with stage data to estimate the cumulative duration of flow above the threshold of motion, which ~~a value that varies in time and space and~~ is ~~therefore~~ difficult to measure directly (Charru et al., 2004). At each seed reach, we used pressure transducer data to identify~~ied~~ the critical flow depth ~~at each reach's pressure transducer~~ (h_c) that ~~pairs~~ corresponds with the R_c for initiating sediment motion, thus linking stage data to estimates of channel-averaged U^* during the 2014 flood hydrograph. Estimates of U^*_e were then integrated across the 2014 hydrograph to estimate I*. Because Eq. (3) is restricted ~~only~~ to flow above the threshold of sediment motion, I* limits the frequency-magnitude distribution of U* to conditions relevant to estimated sediment transport and only considers the momentum excess imparted by the flow on sediment particles. This approach adopts the simplifying assumption of a constant U^*_c for a given field site (after Phillips et al., 2013), although we recognize that U^*_c likely varies in both space and time.

3 Results

~~**3.1 2014 flood hydrology**~~

~~Flow stage at all transducer locations rose sharply around May 1, peaking between May 25 and June 4, depending on the reach (Supplemental Information). The 2014 flood hydrograph at the East Fork Bitterroot seed reach, lower confluence, is shown in Figure 4. Flow stage at different sites exceeded the estimated threshold of incipient motion for 8–37 ($\tau^*_{c,Mueller}$) or 1–17 ($\tau^*_{c,Recking}$) days, with the lower confluence experiencing the longest duration above the critical level. We used the transducer data, along with Parrett and Johnson (2004)regression equations developed for western Montana streams (Parrett and Johnson, 2004) and analysis of a downstream US Geological Survey gauge, to estimate the peak discharge in 2014 as a 3.5 to 4-year event.~~

3.~~2~~ 1 ~~Tracer recovery and displacement~~Field observations of particle displacement

We recovered ~~of 75%~~68–~~to~~ 86% of the seeded tracers, depending on the reach (Table 2). Recovery was greatest within study reaches with low D_{84} values and short transport distances, including the control reach and Moose Creek (Table 2). Our recovery rate is comparable to recent tracer studies using RFID technology: 25–78% (Liébault et al., 2012), 93–98% (Bradley and Tucker, 2012), 62–100% (Phillips et al., 2013), 40% (Chapuis et al., 2015).

Similar percentages of recovered tracers (41, 39, and 50%) left each seed reach. At the upper confluence, tracer configurations within the seed reach retained the signature of their gridded spatial pattern in Moose Creek but not in Martin Creek, which contained more boulders to facilitate trapping and clustering of particle tracers (Figure 5). Particles seeded in Moose Creek also constituted the majority of tracers exported into the confluence itself. Deposition within the confluence primarily correlated to depositional bars flanking the scour hole (Figure 6). Particles deposited within the scour hole were segregated by contributing stream. ~~No tracers from the upper confluence were recovered beyond the extent of the equilibrium confluence morphology in the upper confluence.~~Tracers from the upper confluence seed reaches had short travel distances and, even after being mobilized, remained within the confluence zone (Figure 6).

Particles recovered in the lower confluence largely retained the signature of the gridded arrangement of their initial positioning at both seed reaches, even after mobilization. The relative contribution of tracers into the confluence was more evenly distributed than in the upper confluence: 55% of deposited tracers came from the East Fork, with the remaining 45% from Martin Creek. Similar to the upper confluence, tracer particles remained segregated as they progressed through the confluence, stranding preferentially on bank-attached depositional bars. Deposition within the scour hole was limited and segregated, further agreeing with the upper confluence. An additional group of tracers, seeded at the upstream junction corner, were immobile. Similar to the upper confluence, large boulders were effective in trapping mobile tracer particles. Of the recovered tracers in the entire lower confluence, 23% left the confluence zone completely, with 58% of post-confluence tracers originating in the East Fork and 42% from Martin Creek. Recovered particles downstream of the lower confluence cease to be segregated after about 30 m, and were recovered approximately in the channel center.

~~3.2 Model results~~

3.2 Particle displacement distributions

The Einstein-Hubbell Sayre (EHS) and Yang-Sayre (GEM) models provided similar-quality fits to each other in all study reaches (Figure 7). The Yang-Sayre GEM provides the most accurate fit, with a slight R^2 advantage ranging from 0.01 to 0.001. Both the EHS and GEM models ~~deliver~~ accurately approximate~~ions of~~ the slowest-moving tracer bins, ~~before~~ generally overestimat~~ing~~e the probabilities of mid-range bins, and underestimat~~ing~~e the probabilities of fast-moving bins~~. Fast-moving tracer bins underpredicted by the models~~ that correspond to the tail of the ~~step-length~~displacement probability distribution. In the control reach, fast tracer bins generally have a smaller residual than in the confluence study reaches~~ (Figure 7)~~. The models fit the lower confluence tracers better than the upper confluence tracers (Table 3). In all reaches but Martin Creek (lower confluence), the average transport distance of our data exceeded model estimates (Table 3).

~~3.3 Effects on travel distance~~

~~3.3.1 Tracer dispersion~~

At the upper confluence, mobile tracers entering the confluence zone exhibited a distinct step in the spatial distribution of tracer positions, denoting enhanced transport and reduced depositional probabilities (Figure 8, after Haschenburger, 2013). Enhanced transport is also evident for tracers routing through the lower confluence reaches (Figure 8): a distinct step is evident for tracers entering the confluence, where the probability of deposition decreases for the duration of time spent within the confluence zone. ~~Compared to the confluence reaches, t~~The control reach lacks significant steps and instead features a smooth decay indicative of consistent depositional rates~~.~~.

Dimensionless ~~step-length~~displacement distributions deviate from a best-fit exponential distribution at distances beyond approximately twice the average normalized transport distance (Figure 9). In evaluating X_n, tracers in the upper confluence reaches do not travel as far relative to the population mean as those in other seed reaches. ~~When we assessed tail~~Tail character in~~,~~ confluence populations generally showed smaller α values than the control reach, corresponding to heavier tails and greater dispersive growth (Figure 10). ~~However, t~~The point of origin of the tail is user-defined, however, and varying the start point changes the resulting slope of the exceedance tail. We therefore assessed tail character at multiple points above the 75th percentile of tracer displacement distance, to test the sensitivity of tail designation ~~(thin or heavy)~~. None of the study reaches cross the thin-heavy threshold (α=2) by varying the tail start point, though α values are sensitive. We thus chose to define~~settle for defining~~ the tail as beginning at the 80th tracer percentile ~~(Figure 10)~~. Only Moose Creek shows a thinner tail in the exceedance probability distribution than the control reach. Martin Creek (at both the upper and lower confluences) exhibits a heavy-tail, while Moose Creek, the control reach, and East Fork Bitterroot are thin-tailed. The data do not distinguish ~~on~~ whether transport through confluences is thin or heavy-tailed, rather suggesting that distributions of tracers moving through confluences are generally "heavier" and exhibit a higher proportion of tracers traveling far distances than in the plane-bed reach.

~~3. Grain size and travel distance~~

~~Comparison of our transport data, represented in terms of scaled travel distance and scaled tracer size, Figure 11 shows our tracer transport data, among 10-mm subsets from 60 to 130 mm particles, compared to Eq. 2 (Church and Hassan, 1992)'s empirical relationship for provides a means of evaluating whether tracer displacements showed size-dependent transport characteristics (Figure 11 (Eq. 2). The control reach tracers were largely characterized byagreed with size-selective transport characteristics, with the largest residual relative to the curve occurring for the largest grain-size bins, which experienced shorter transport distances than what would be expected from Eq. (2). The two confluence sites showed worse agreement to the empirical curve of Church and Hassan (1992). The upper confluence shows nearly equal transport distances across all grain-size bins, while the lower confluence data show a peak in mobility for particle sizes around the tracer median.~~

3.3 Dimensionless impulse

Our estimates of critical Shields number ranged from 0.056 to 0.109 (Table 4), slightly larger than often-assumed values of τ_c^* (e.g., τ_c^*=0.045; Church, 2006). For all study reaches, $\tau^*_{c,Mueller}$ values (Eq. 5) were lower than the $\tau^*_{c,Recking}$ values (Eq. 6), ~~predicting~~ resulting in correspondingly lower U^*_c values. These calculations indicate that ~~F~~flow exceeded the threshold of ~~incipient~~ motion for 8–37 ($\tau^*_{c,Mueller}$) or 1–17 ($\tau^*_{c,Recking}$) days, with the lower confluence experiencing the longest duration above the critical level. -The distribution of U* and I* scale~~s~~ with channel dimensions and peak discharge, with the upstream confluence seed reaches experiencing smaller U* and I* values than the control reach and lower confluence (Table 4). ~~As I* depends on the estimated threshold of motion for each study reach, itself a function of grain size and hydraulic radius, we note a reliance of I* on channel roughness. The difference between I* estimates also varies as a function of hydraulic radius.~~ Moose Creek, for example, is wider and shallower than Martin Creek at the upper confluence, and requires a larger discharge increase to move from the Mueller to Recking incipient motion threshold estimate. This results in reach-specific variation in sensitivity to the estimation method for incipient motion. We found that I* scaled well with tracer displacement (Table 4) and confirmed its usefulness for assessing coarse particle transport at the EFB.

We found <X/D> to conform to a linear relation to I*, and variance (σ^2) to a power-law function, in agreement to the predictions and findings of Phillips et al. (2013) and Phillips and Jerolmack (2014) regarding the broad applicability of normalized travel distances and impulse for characterizing bedload transport (Figure 11). The occurrence of a linear fit supports the notion that I* may be used to correlate flow strength with travel distance across multiple sites. However, a linear fit through the origin was far less appropriate than that found by Phillips et al. (2013). Fits could be greatly improved when only considering the relationship between confluence reaches: the control reach has similar displacement but higher I* values than reaches at the upper confluence, giving it the highest residual from the best-fit curve in both cases. We did not normalize I* by frictional resistance, as it did not prove to significantly improve the collapse of our tracer data.

4 Discussion

4.1 Coarse -sediment routing through confluences

Our study used PIT / RFID technology to provide novel insights into the effect of tributary confluences on sediment routing through mountain streams. Maximum transport distances along scour-hole flanks and segregation are similar to the findings of Mosley (1976) and Best (1988). Because we detect no tracers beyond the extent of the upper confluence, we take the depositional pattern in Figure 6 to reflect a tendency of our tracers to route along, rather than through, the scour hole. We ~~do not know how tracers recovered beyond the lower confluence progressed through the confluence itself, but we~~ see similar depositional patterns for tracers that were detected within the lower confluence and posit that similar transport corridors apply. We consider these transport patterns to reflect the controlling influences of Θ and Q_r; the simple upstream planform geometry and minimal bed discordance (z_d) at our sites suggest that tho~~e~~se factors ~~have less~~exert little influence on ~~confluence~~ morphodynamics ~~of~~in our study confluences. Observed discordance between scour and tributary mouth bars at our study confluences (0.6 and 1.4 m, respectively) exceed that of Roy and Bergeron (1990; ~0 m at Θ=15), supporting observations that scour is largely absent at low Θ values (Benda and Cundy, 1990).

Our data also agree with the assertions of Best (1988) and others as to how the position and orientation of the scour hole is influenced by Q_r. Increased penetration of flow from the tributary at the upper confluence, due to higher Q_r, forced the scour hole towards the middle of the confluence, as opposed to the lower confluence where the scour was shifted by greater discharge from the East Fork Bitterroot. Observed feedbacks between confluence morphology and particle transport suggest similar confluence morphodynamics as observed in past studies (e.g., Mosley, 1976; Best, 1987; Boyer et al., 2006; Rhoads et al., 2009), though in a higher-gradient, more headwaters setting than previous work.

4.2 Effects of confluences on dispersion

Fit quality of the EHS and GEM models support Bradley and Tucker's (2012) assertion that a gamma or exponential distribution can approximate the ~~true~~ compound Poisson distribution of coarse tracer displacement in headwater systems. ~~The monotonically decreasing nature of the EHS is likely responsible for inferior fits relative to the GEM, similar to the observations of Bradley and Tucker (2012), though d~~Differences between the EHS and GEM~~two~~ at our site are almost indistinguishable, whereas Bradley and Tucker (2012) found that the GEM described observed step lengths than the monotonically decreasing EHS. ~~. We can only assume t~~The strong fits of the EHS and GEM may reflect the ~~to provide adequate fits over~~ short duration (one flood) of our study; ~~time periods, as our work and that of~~ Bradley and Tucker (2012)'s study spanned four ~~cover 1 and 4~~ flood events~~, respectively~~. The quality of these fits is likely to weaken over time as particles become vertically integrated with the bed (Haschenburger, 2013).

General accordance to the EHS and GEM models suggests that a thin-tailed model may be reasonable for describing particle displacement distributions through confluences as well as in our control reach. The linear collapse in semi-log space observed in Figure 9 further supports this view, indicating that normalized transport distance (Eq. 1) may serve as an appropriate single-parameter approach to describe tracer displacement at the scale of individual floods. However, the tail of the distribution ~~exhibits considerable~~ diverges~~nce~~ from the model fits and exponential regression. This divergence is evident in our other analyses, which suggest relatively heavy-tailed displacement distributions and reduced depositional probabilities for coarse sediment within the confluence zone. Enhanced transport is further suggested by larger transport distances for a given impulse (Table 4; Figure 10). We therefore assert that coarse particles entering the confluence zone are less likely to deposit than in the preceding plane bed reach, and that particles exposed to the greater dimensionless impulse beyond the confluence travel fa~~u~~rther distances than those that do not enter the confluence.

4.3 Confluences and large-scale sediment routing

We therefore propose a conceptual model where equilibrium confluences have the effect of enhancing coarse bedload transport and dispersion downstream. Tracers moving through confluences show greater transport distances for a given I* and reduced depositional probabilities in the confluence itself. This would distort the spatial distribution of a population of coarse particles in the Lagrangian field perspective, where front-runner tracers are preferentially routed through confluences and the overall spatial distribution distorted in the downstream direction. ~~While~~Tracer transport dynamics were reasonably well-fitted by thin-tailed models, but not for far-traveling tracers. The differences we observe between confluence and non-confluence reaches are subtle, ~~model fits were not greatly different between control and confluence reaches,~~

~~we expect this effect to increase in significance as coarse particles are routed through multiple~~ but this effect may increase as particles are routed through successive confluences.

This conceptual model applies to confluence morphology that is governed by hydraulics and sediment supply typical of snowmelt-dominated hydrographs, as opposed to confluences influenced by recent disturbance. We consider our model within the context of Benda et al.'s (2004) Network Variance Model, to consider the effects of confluences at the scale of headwater river networks. The NVM considers that the likelihood of morphologically significant perturbations to mainstem channels, in the form of large sediment deposits, increases in the vicinity of confluences due to upstream disturbance. Our sites, where recent tributary disturbances are absent, diverge from this model, such that sediment can propagate, unhindered by ~~past~~ recent sediment deposits, through confluence zones, and indeed, transport is enhanced rather than impeded across our equilibrium confluences. Our work expands, rather than refutes, the NVM by suggesting that confluences play morphologically important roles with respect to sediment routing both in and outside of disturbance-dominated headwater systems.

We hypothesize, based on our findings above, that sediment routing through individual equilibrium confluences influences routing at the larger basin scale in mountain watersheds. As the equilibrium confluence is contingent on high Q_r, Θ, and other physical controls, we would expect certain basin types to accumulate confluence effects to a greater extent than others, according to basin shape, drainage density, and network geometry (Benda et al., 2004). As an illustrative example, we compare the EFB basin to a similarly sized basin (Tin Cup Creek), 35 km to the west in the ~~nearby~~ Bitterroot Range (Figure ~~13~~12). The morphology of basins in the Bitterroot versus Sapphire Mountains differs considerably as a result of differences in erosive history and lithology. The Bitterroot are formerly glaciated and have granitic rock, with U-shaped valleys, elongate basins, and trellis drainage networks. The unglaciated Sapphires, in contrast, have V-shaped valleys, compact basins, and dendritic networks. Comparing these basin types, basins such as those in the Sapphire Range (e.g., the upper EFB basin) have larger tributary channels of increasing order (Strahler, 1952), where tributary discharges scale with increased mainstem flow, and a greater number and downstream extent of equilibrium confluences than the elongate basins (Benda et al., 2004) ~~like those~~that largely define basins such as ~~in~~ the Bitterroot. ~~Other basin factors, such as network geometry and distance between equilibrium confluences, are further expected to govern confluence effects on nonlocal sediment routing (Benda et al., 2004).~~ This suggests that basin shape, itself a function of lithology and climate, may ~~provide~~ inform~~ation regarding~~ the dispersive behavior of a coarse bedload population in locations ~~absent of~~lacking recent disturbance and corresponding confluence deposits. This would~~,~~ determine~~ing~~ the setting where confluences would be expected to enact a cumulative and significant effect on coarse sediment transport.

Understanding the extent to which equilibrium confluences affect basin-scale routing requires further insight into coarse bedload connectivity in mountain rivers. Our conceptual model assumes steady progression of coarse sediment downstream in a plane-bed morphology; however, discontinuity in coarse sediment transfer can emerge when competence is reduced and particles enter long-term storage (e.g., Tooth et al., 2002; Hooke, 2003; Fryirs, 2013; Bracken et al., 2015). Certain channel morphologies exhibit bedload particle displacements between morphologic units (e.g., bars; Pyrce and Ashmore, 2003), which can result in disconnectivity if bedform-scale aggradation exceeds rates of removal (Hooke, 2003). ~~Ultimately, th~~The unique dispersive patterns we observe at the scale of individual confluences must be analyzed ~~cumulatively,~~ across multiple confluences, over multiple floods, and within other channel morphologies, to quantify the extent of their influence over large-scale patterns of sediment routing.

5 Conclusion

Our tracer study, the first to date of coarse-sediment routing through mountain-river confluences, showed that in gravel-bed headwater systems, tributary confluences represent geomorphically unique locations that locally affect patterns of sediment routing. At the reach scale, coarse sediment is routed through confluences along the flanks of a well-defined scour hole, in agreement with observations and flume studies from other gravel-bed systems. Transport distance of mobilized clasts through the confluence zone is less dependent on grain size than in the plane-bed channel morphology, especially for larger grains. Distributions of particle displacement were along the thin-heavy tail threshold; longer-term monitoring would elucidate the evolution of tail characteristics. Regardless of thin or heavy-tailed transport, confluence reaches generally featured a "heavier" distribution of displacement distances and a greater proportion of tracers in the tail. ~~We~~ We therefore found confluence reaches to impart greater transport distances and dispersive growth compared to the plane-bed channel morphology, even when particles did not progress beyond the downstream extent of the confluence itself. Our study also illustrates the utility of tracer studies using PIT / RFID technology for providing field-based insights into sediment transport dynamics.

We proposed a conceptual model where equilibrium headwater confluences ~~promote enhanced~~alter patterns of dispersion and ~~impart greater~~enhance downstream transport ~~distances than otherwise expected~~. According to the sediment cascade framework of Fryirs (2013), this would classify equilibrium confluences as an enhanced longitudinal linkage compared to the plane-bed channel morphology. ~~The conceptual model posited herein adds to previous study by suggesting that sediment routing through fluvially dominated confluences alters overall particle dispersion.~~ Combined with the work of Benda et al. (2004) and others, we suggest that the location of confluences influences sediment routing patterns and, in the case of upstream disturbances, responses to sediment pulses, in headwater systems both with and without disturbance-derived sediment deposits. Longer-term sediment transport studies across confluence and non-confluence reaches, combined with analysis of changes in bed elevation and texture in intervening reaches to place the work in a mass conservation framework, would further clarify sediment routing patterns in mountain channel networks and thus inform ~~These results pertain to~~ a range of problems ~~in headwater networks~~, including solid-phase contaminant transport (Bradley et al., 2010), cosmogenic radionuclide accumulation (Gayer et al., 2008), sediment budgeting (Malmon et al., 2005), and the duration and topographic impact of pulses on aquatic habitat (Lisle et al., 2001).

Acknowledgments

We thank P.A. Duvillard, A. Maphis, D. Davis, M. Jahnke, and A. Sawyer for field ~~exceptional~~ assistance; ~~during the 2014 field season. We thank~~ M. Hassan, L. Eby, M. Maneta, S. Bywater-Reyes, and R. Manners for ~~valuable~~ insight in the planning and implementation of this work; ~~.~~

~~We thank~~ N. Bradley and C. Legleiter for aid in model use and coordinate transformation; and~~.~~ ~~We thank~~ C. Phillips for assistance in performing impulse analyses. Comments from two anonymous reviewers greatly improved the manuscript. This work was supported by the Montana Institute on Ecosystems' award from the National Science Foundation EPSCoR Track-1 program under Grant # EPS-1101342, and~~. This work was also supported~~ by ~~grants from~~ the Montana Geological Society, the Geological Society of America, and the Northwest Scientific Association.

References

Ashmore, P. and Parker, G.: Confluence scour in coarse braided streams, Water Resour. Res., 19, 392–402, 1983.

Benda, L. and Cundy, W.: Predicting deposition of debris flows in mountain channels, Can. Geotech. J., 27, 409–417, 1990.

Benda, L. and Dunne, T.: Stochastic forcing of sediment routing and storage in channel networks, Water Resour. Res., 33, 2865–2880, 1997.

Benda, L., Andras, K., Miller, D., and Bigelow, P.: Confluence effects in rivers: Interactions of basin scale, network geometry, and disturbance regimes, Water Resour. Res., 40, W05402, doi:10.1029/2003WR002583, 2004.

Best, J.: Flow dynamics at river channel confluences: implications for sediment transport and bed morphology, Soc. Econ. Paleontol. Minearologists, 39, 27–35, 1987.

Best, J.: Sediment transport and bed morphology at river channel confluences, Sedimentology, 35, 481–498, 1988.

Best, J.L., and Rhoads, B.L.: Sediment transport, bed morphology and the sedimentology of river channel confluences, in: River Confluences, Tributaries and the Fluvial Network, JohnWiley and Sons, Chichester, UK, 2008.

Biron, P., Best, J.L., Roy, A.G.: Effects of bed discordance on flow dynamics at open channel confluences, J. Hydraul. Eng., 122, 676–682, 1996.

Boyer, C., Roy, A.G., and Best, J.: Dynamics of a river channel confluence with discordant beds: Flow turbulence, bed load sediment transport, and bed morphology, J. Geophys. Res., 111, F04007, doi:10.1029/2005JF000458, 2006.

Bracken, L. J., Turnbull, L., Wainwright, J. and Bogaart, P.: Sediment connectivity: a framework for understanding sediment transfer at multiple scales, Earth Surf. Process. Landforms, 40, 177–188, doi:10.1002/esp.3635, 2015.

Bradley, N. and Tucker, G.E.: Measuring gravel transport and dispersion in a mountain river using passive radio tracers, Earth Surf. Process. Landf., 37,1034–1045, doi:10.1002/esp.3223, 2012.

Bradley, D.N., Tucker, G.E., and Benson, D. A.: Fractional dispersion in a sand bed river. J. Geophys. Res., 115, F00A09, doi:10.1029/2009JF001268, 2010.

Brooks, A. and Brierley, G.: Geomorphic responses of lower Bega River to catchment disturbance, 1851-1926, Geomorphology, 18, 291-304, 1997.

Chapuis, M., Bright, C.J., Hufnagel, J., and MacVicar, B.: Detection ranges and uncertainty of passive Radio Frequency Identification (RFID) transponders for sediment tracking in gravel rivers and coastal environments, Earth Surf. Process. Landf., 39, 2109–2120, doi:10.1002/esp.3620, 2014.

Chapuis, M., Dufour, S., Provansal, M., Couvert, B., and de Linares, M.: 2015. Coupling channel evolution monitoring and RFID tracking in a large, wandering, gravel-bed river: Insights into sediment routing on geomorphic continuity through a riffle–pool sequence, Geomorphology, 231, 258–269, doi:10.1016/j.geomorph.2014.12.013, 2015.

Charru, F., Mouilleron, H., and Eiff, O.: Erosion and deposition of particles on a bed sheared by a viscous flow, J. Fluid Mech., 519, 55–80, doi:10.1017/S0022112004001028, 2004.

Church, M.: Geomorphic thresholds in riverine landscapes, Freshw. Biol., 47, 541–557, doi:10.1046/j.1365-2427.2002.00919.x, 2002.

Church, M.: Bed material transport and the morphology of alluvial river channels, Annu. Rev. Earth Planet. Sci., 34, 325–354, doi:10.1146/annurev.earth-33.092203.122721, 2006.

~~Church, M. and Hassan, M. A.: Size and distance of travel of unconstrained clasts on a streambed, Water Resour. Res., 28, 299–303, doi:10.1029/91 WR-02523, 1992.~~

Constantinescu, G., Miyawaki, S., Rhoads, B. L., and Sukhodolov, A.: Numerical analysis of the effect of momentum ratio on the dynamics and sediment-entrainment capacity of coherent flow structures at a stream confluence, J. Geophys. Res., 117, F04028, doi:10.1029/2012JF002452, 2012.

Einstein, H.A.: Bed load transport as a probability problem, Ph.D., ETH Zurich, 1937.

Ferguson, R. and Wathen, S.: Tracer-pebble movement along a concave river profile : Virtual velocity in relation to grain size and shear stress transport and deposition, Water Resour. Res., 34, 2031–2038, 1998.

Ferguson, R., Cudden, J.R., Hoey, T.B., and Rice, S.P.: River system discontinuities due to lateral inputs: generic styles and controls, Earth Surf. Process. Landforms, 31, 1149–1166, doi:10.1002/esp.1309, 2006.

Fryirs, K.: (Dis)Connectivity in catchment sediment cascades: a fresh look at the sediment delivery problem, Earth Surf. Process. Landf., 38, 30–46, doi:10.1002/esp.3242, 2013.

Gayer, E., Mukhopadhyay, S., and Meade, B.J.: Spatial variability of erosion rates inferred from the frequency distribution of cosmogenic 3He in olivines from Hawaiian river sediments, Earth Planet. Sci. Lett., 266, 303–315, doi:10.1016/j.epsl.2007.11.019, 2008.

Gomi, T., Sidle, R.C., and Richardson, J.S.: Understanding processes and downstream linkages of headwater systems, Bioscience, 52, 905-916, doi:10.1641/00063568(2002)052[0905:UPADLO]2.0.CO;2, 2002.

Haschenburger, J.K.: Tracing river gravels: Insights into dispersion from a long-term field experiment, Geomorphology, 200, 121–131, doi:10.1016/j.geomorph.2013.03.033, 2013.

Hassan, M.A., Church, M., and Schick, A.P.: Distance of movement of coarse particles in gravel bed streams, Water Resour. Res., 27, 503–511, 1991.

Hassan, M. A., Voepel, H., Schumer, R., Parker, G., and Fraccarollo, L.: Displacement characteristics of coarse fluvial bed sediment, J. Geophys. Res. Earth Surf., 118, 155–165, doi:10.1029/2012JF002374, 2013.

Hoffman, D.F. and Gabet, E.J.: Effects of sediment pulses on channel morphology in a gravel-bed river, Geol. Soc. Am. Bull., 119, 116–125, doi:10.1130/B-25982.1, 2007.

Hubbell, D. and Sayre, W.: Sand transport studies with radioactive tracers, J. Hydraul. Div., 90, 39–68, 1964.

Imhoff, K.I.: Sediment routing through channel confluences: Particle tracing in a gravel-bed river headwaters, M.S. thesis, University of Montana, Missoula, MT, 2015.

Kasprak, A., Wheaton, J.M., Ashmore, P.E., Hensleigh, J.W., and Peirce, S.: The relationship between particle travel distance and channel morphology : Results from physical models of braided rivers, J. Geophys. Res. Earth Surf., 120, 55–74, http://doi:10.1002/2014JF003310, 2014.

Knighton, A.D.: Longitudinal changes in size and sorting of stream-bed material in four English rivers, Geol. Soc. Am. Bull., 91, 55-62, 1980.

Lajeunesse, E., Malverti, L., and Charru, F.: Bed load transport in turbulent flow at the grain scale: Experiments and modeling, J. Geophys. Res., 115, F04001, doi:10.1029/2009-JF001628, 2010.

Lamarre, H. and Roy, A.G.: The role of morphology on the displacement of particles in a step–pool river system, Geomorphology, 99, 270–279, doi:10.1016/j.geomorph.2007.11.005, 2008.

Lamarre, H., MacVicar, B., and Roy, A. G.: Using passive integrated transponder (PIT) tags to investigate sediment transport in gravel-bed rivers, J. Sediment. Res., 75, 736–741, doi:10.2110/jsr.2005.059, 2005.

Lancaster, S.T. and Casebeer, N.E.: Sediment storage and evacuation in headwater valleys at the transition between debris-flow and fluvial processes, Geology, 35, 1027-1030, doi:10.1130/G239365A.1, 2007.

Liébault, F., Bellot, H., Chapuis, M., Klotz, S., and Deschâtres, M.: Bedload tracing in a high-sediment-load mountain stream, Earth Surf. Process. Landforms, 37, 385–399, doi:10.1002/esp.2245, 2012.

Lisle, T.E., Cui, Y., Parker, G., Pizzuto, J.E., and Dodd, A.M.: The dominance of dispersion in the evolution of bed material waves in gravel-bed rivers, Earth Surf. Process. Landforms, 26, 1409–1420, doi:10.1002/esp.300, 2001.

Malmon, D. V., Reneau, S.L., Dunne, T., Katzman, D., and Drakos, P.G.: Influence of sediment storage on downstream delivery of contaminated sediment, Water Resour. Res., 41, 1–17, doi:10.1029/2004WR003288, 2005.

Martin, R. L., Jerolmack, D.J., and Schumer, R.: The physical basis for anomalous diffusion in bed load transport, J. Geophys. Res., 117, F01018, doi:10.1029/2011JF002075, 2012.

Metzler, R., and Klafter, J.: The random walk's guide to anomalous diffusion: a fractional dynamics approach, Physics Reports, 339, 1-77, doi:10.1016/S0370-1573(00)000703, 2000.

Milan, D. J.: Sediment routing hypothesis for pool-riffle maintenance, Earth Surf. Process. Landforms, 38, 1623–1641, doi:10.1002/esp.3395, 2013.

Montgomery, D. R and Buffington, J.M.: Channel-reach morphology in mountain drainage basins, Geol. Soc. Am. Bull., 109, 596–611, 1997.

Mosley, M.P.: An experimental study of channel confluences, J. Geol., 84, 535–562, 1976.

Mueller, E.R., Pitlick, J., and Nelson, J.M.: Variation in the reference Shields stress for bed load transport in gravel-bed streams and rivers, Water Resour. Res., 41, F02016, doi:10.1029/2004WR003692, 2005.

Nikora, V., Habersack, H., Huber, T., and McEwan, I.: On bed particle diffusion in gravel bed flows under weak bed load transport, Water Resour. Res., 38, 9 pp., doi:200210.1029/2001WR000513, 2002.

Olinde, L., and Johnson, J.P.L.: Using RFID and accelerometer-embedded tracers to measure probabilities of bed load transport, step lengths, and rest times in a mountain stream, Water Resour. Res., 51, 7572-7589, doi:10.1002/2014WR016120, 2015.

Parrett, C., and Johnson, D.R.: Methods for estimating flood frequency in Montana based on data through water year 1998, USGS Water-Resources Investigations Rep. 03-4308, Reston, VA, 2004.

Phillips, C.B. and Jerolmack, D.J.: Dynamics and mechanics of bed-load tracer particles, Earth Surf. Dyn., 2, 513–530, doi:10.5194/esurf-2-513-2014, 2014.

Phillips, C.B., Martin, R.L., and Jerolmack, D.J.: Impulse framework for unsteady flows reveals superdiffusive bed load transport, Geophys. Res. Lett., 40, 1328–1333, doi:10.1002/grl.50323, 2013.

Prosser, I.P., Rutherfurd, I.D., Olley, J.M., Young, W.J., Wallbrink, P.J., and Moran, C.J.: Large-scale patterns of erosion and sediment transport in river networks, with examples from Australia, Mar. Freshw. Res., 52, 81–99, doi:10.1071/MF00033_CO, 2001.

Pyrce, R. S., and Ashmore, P.E.: The relation between particle step length distributions and channel morphology in gravel-bed streams: a synthesis, Geomorphology, 56, 167–187, doi:10.1016/S0169-555X(03)00077-1, 2003.

Recking, A.: Simple method for calculating reach-averaged bed-load transport, J. Hydraul. Eng., 139, 70–75, doi:10.1061/(ASCE)HY.1943-7900.0000653, 2013.

Rhoads, B.L.: Changes in stream channel characteristics at tributary junctions. Phys. Geogr., 8, 346–361, doi:10.1080/02723646.1987.10642333, 1987.

Rhoads, B.L. and Sukhodolov, A.N.: Spatial and temporal structure of shear layer turbulence at a stream confluence, Water Resour. Res., 40, doi:10.1029/2003WR002811, 2004.

Rhoads, B.L., Riley, J.D., and Mayer, D.R.: Response of bed morphology and bed material texture to hydrological conditions at an asymmetrical stream confluence, Geomorphology, 109, 161–173, doi:10.1016/j.geomorph.2009.02.029, 2009.

Ribeiro, M.L., Blanckaert, K., Roy, A. G., and Schleiss, A. J.: Flow and sediment dynamics in channel confluences, J. Geophys. Res., 117, F01035, doi:10.1029/2011JF002171, 2012.

Rice, S.P., Greenwood, M.T., and Joyce, C.B.: Tributaries, sediment sources, and the longitudinal organisation of macroinvertebrate fauna along river systems, Can. J. Fish. Aquat. Sci., 58, 824–840, doi:10.1139/cjfas-58-4-824, 2001.

Richards, K.S.: A note on changes in channel geometry at tributary junctions, Water Resour. Res., 16, 241–244, doi:10.1029/WR016i001p00241, 1980.

Roy, A.G. and Bergeron, N.: Flow and particle paths at a natural river confluence with coarse bed material, Geomorphology, 3, 99–112, doi:10.1016/0169555X(90)90039S, 1990.

Sklar, L. S., Fadde, J., Venditti, J.G., Nelson, P., Wydzga, M.A., Cui, Y., and Dietrich, W.E.: Translation and dispersion of sediment pulses in flume experiments simulating gravel augmentation below dams, Water Resour. Res., 45, W08439, doi:10.1029/2008WR007346, 2009.

Strahler, A.N.: Hypsometric (area-altitude) analysis of erosional topography, Geol. Soc. Am. Bull., 63, 1117-1142, doi:10.1130/00167606(1952)63[1117:HAAOET]2.0.CO;2, 1952.

Swanson, F.J. and Fredriksen, R.L.: Sediment routing and budgets : Implications for judging impacts of forestry practices, in: Sediment Budgets and Routing in Forested Drainage Basins, Swanson, F.J., Janda, R.J., Dunne, T., Swanston, D.N., U.S. Forest Service, Portland, OR, 129-137, 1982.

Swanson, B. J., and Meyer, G.: Tributary confluences and discontinuities in channel form and sediment texture: Rio Chama, NM, Earth Surf. Process. Landforms, 39, 1927–1943, doi:10.1002/esp.3586, 2014.

Tooth, S., McCarthy, T.S., Brandt, D., Hancox, P.J., and Morris, R.: Geological controls on the formation of alluvial meanders and floodplain wetlands: the example of the Klip River, eastern Free State, South Africa, Earth Surf. Process. Landforms, 27, 797–815, doi:10.1002/esp.353, 2002.

Yang, C. and Sayre, W.: Stochastic model for sand dispersion. J. Hydraul. Div., 97, 265–288, 1971.

Tables

Table 1: Channel morphology and bed-material ~~Geometric and~~ grain-size characteristics ~~of the bed~~ at each study reach. Width and depth values are ~~at~~ bankfull dimensions, as measured along surveyed~~the~~ cross-sections; Q_r, θ, and z_d are illustrated and defined in Figure 1 ~~taken at each location~~. Upper and lower confluences reaches are denoted with (U) and (L), respectively.

Study Reach	**S**	**Width (m)**	**Depth (m)**	**D_{50} (m)**	**D_{84} (m)**	**Q_r[a] (avg)**	**Θ**	**z_d (m)**
Moose Creek (U)	0.018	11	0.76	0.05	0.10	0.63	86°	0.16
Martin Creek (U)	0.029	7	0.94	0.06	0.15			
Control Reach	0.016	15	0.78	0.06	0.13	–	–	–
Martin Creek (L)	0.017	15	0.80	0.07	0.12	0.45	81°	0
East Fk. Bitterroot (L)	0.016	16	1.03	0.07	0.14			

[a] calculated by dividing the smaller trunk stream by volume over the mainstem. Qr = Q(Moose)/Q(Martin) in the upper confluence, and Q(Martin)/Q(East Fork) in the lower confluence.

Table 2: Tracer recovery and transport statistics by study reach

Study Reach	**n**[a]	**n_{rec}**[b]	**Recovery (%)**	**D_{50} (m)**	**$(X \pm \sigma)_{tot}$ (m)**[c]	**$(X \pm \sigma)_{mob}$ (m)**	**X_{max} (m)**
Moose Creek (U)	65	53	82	0.077	7.4$\pm$6.6	8.5$\pm$6.4	24.5
Martin Creek (U)	62	42	68	0.081	3.8$\pm$4.1	4.4$\pm$4.1	20.6
Control Reach	97	83	86	0.080	4.2$\pm$5.3	4.9$\pm$5.4	22.7
Martin Creek (L)	103	71	68	0.082	14.6$\pm$22.9	16.4$\pm$24	133
East Fk. Bitterroot (L)	101	74	73	0.080	47.4$\pm$56.3	49.4$\pm$56.6	211

[a] number of tracers deployed

[b] number of tracers recovered

[c] X is average transport distance, σ is standard deviation

* “tot” and “mob” describe (1) the total tracer population and (2) tracers moving beyond 0.5 meters

Table 3: ~~Model-derived t~~Tracer statistics derived from two stochastic models of tracer transport and dispersion: Einstein-Hubbell-Sayre (EHS) and the Yang-Sayre Gamma Exponential Model (GEM).

	EHS			**GEM**		
Study Reach	**X**	**σ**	**CV**[a]	**X**	**σ**	**CV**
Moose Creek (U)	6.7	5.7	0.86	6.6	5.7	0.87
Martin Creek (U)	3.8	3.8	1.0	3.8	3.9	1.0
Control Reach	4.2	4.6	1.1	4.2	4.6	1.1
Martin Creek (L)	15.6	24.6	1.6	16.2	25.1	1.6
East Fk. Bitterroot (L)	43.9	61.4	1.4	43.7	61.0	1.4

[a] coefficient of variation

[b] The values presented here incorporate estimates of critical Shields stress calculated from Eq. 4 (Mueller et al., 2005); results are nearly identical if Eq. 6 is used instead.

Table 4: Critical shear velocity (U_c*) and dimensionless impulse (I*) at each study reach.

	$\tau^*_{c,Mueller}$			$\tau^*_{c,Recking}$		
Study Reach	τ^*_c	U^*_c **(m/s)**	I^*	τ^*_c	U^*_c **(m/s)**	I^*
Moose Creek (U)	0.06	0.23	602000	0.08	0.27	14900
Martin Creek (U)	0.08	0.29	310000	0.11	0.34	37600
Control Reach	0.06	0.23	425000	0.07	0.25	88400
Martin Creek (L)	0.06	0.25	1200000	0.09	0.31	86000
East Fk. Bitterroot (L)	0.06	0.25	1900000	0.07	0.29	577000

Figures

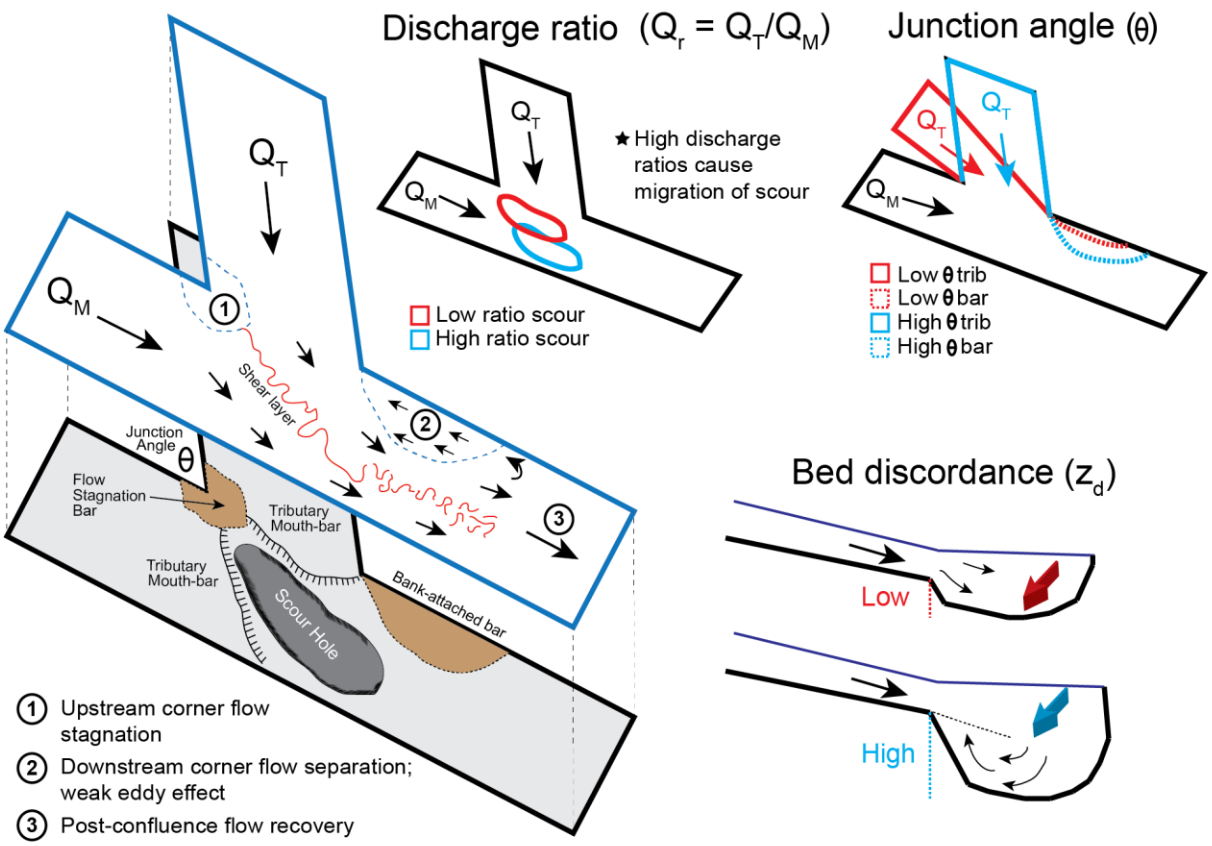

Figure 1: Flow (top left) and morphology (bottom left) in a gravel-bed confluence (after Best, 1987). Key variables influencing hydraulics and morphology include discharge ratio (Q_r), junction angle (θ), bed discordance (z_d), and upstream planform geometry (not pictured).

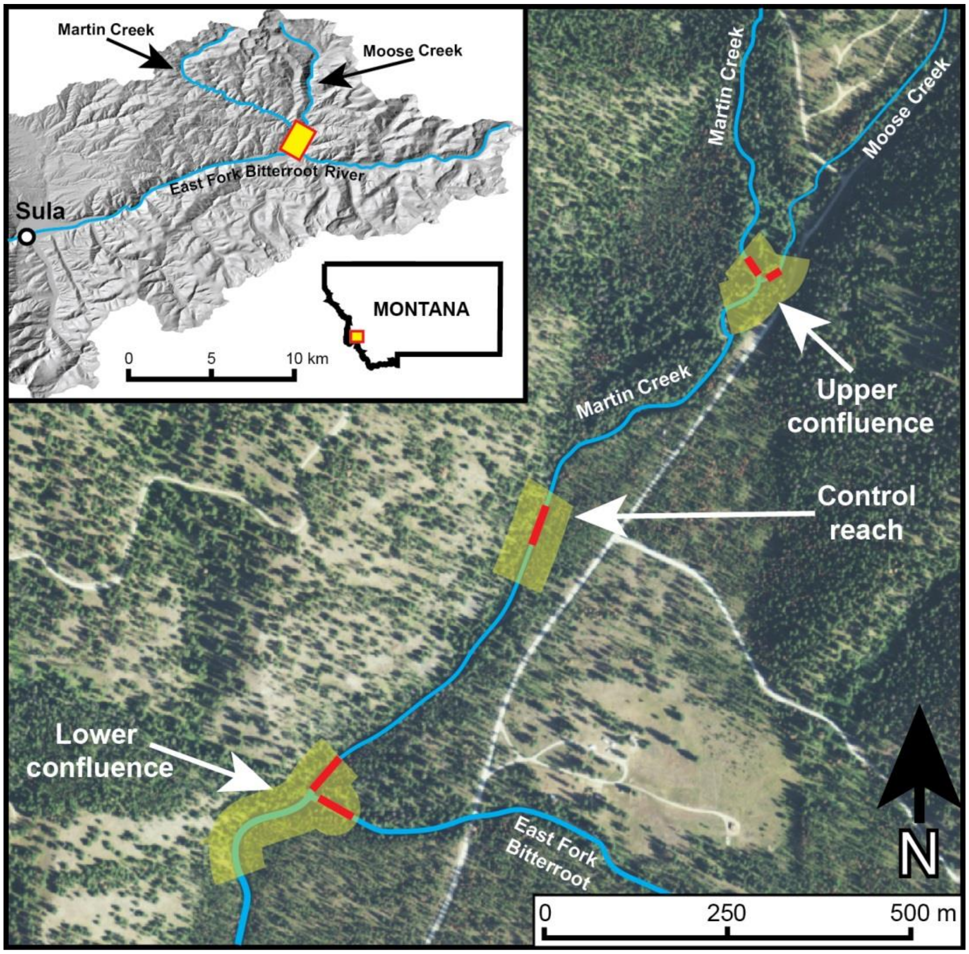

Figure 2: Study area, including location within the East Fork Bitterroot River's headwaters (upper left) and three study sites: upper and lower confluences and a control reach, outlined in yellow; individual reaches in which PIT-tagged particles were seeded are outlined in red.

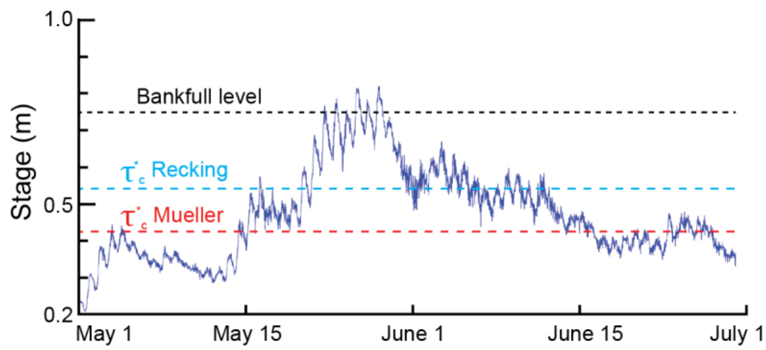

Figure 43: Stage hydrograph during spring 2014 runoff period at lower confluence (East Fork Bitterroot River) study site. Estimated bankfull level, based on cross-section topography surveyed at transducer location, is shown as horizontal dotted line.

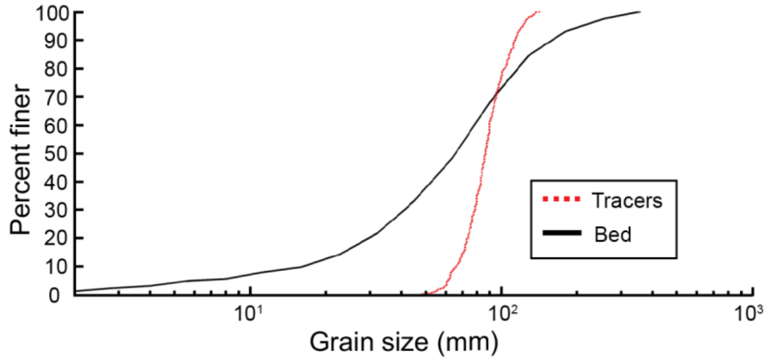

Figure ~~3~~4: ~~(A) ~~Grain size distribution of tagged tracers (red) ~~as compared to the~~and streambed (black) composite over all study sites. ~~Below are photographs of the (B) upper confluence, (C) control reach, and (D) lower confluence.~~

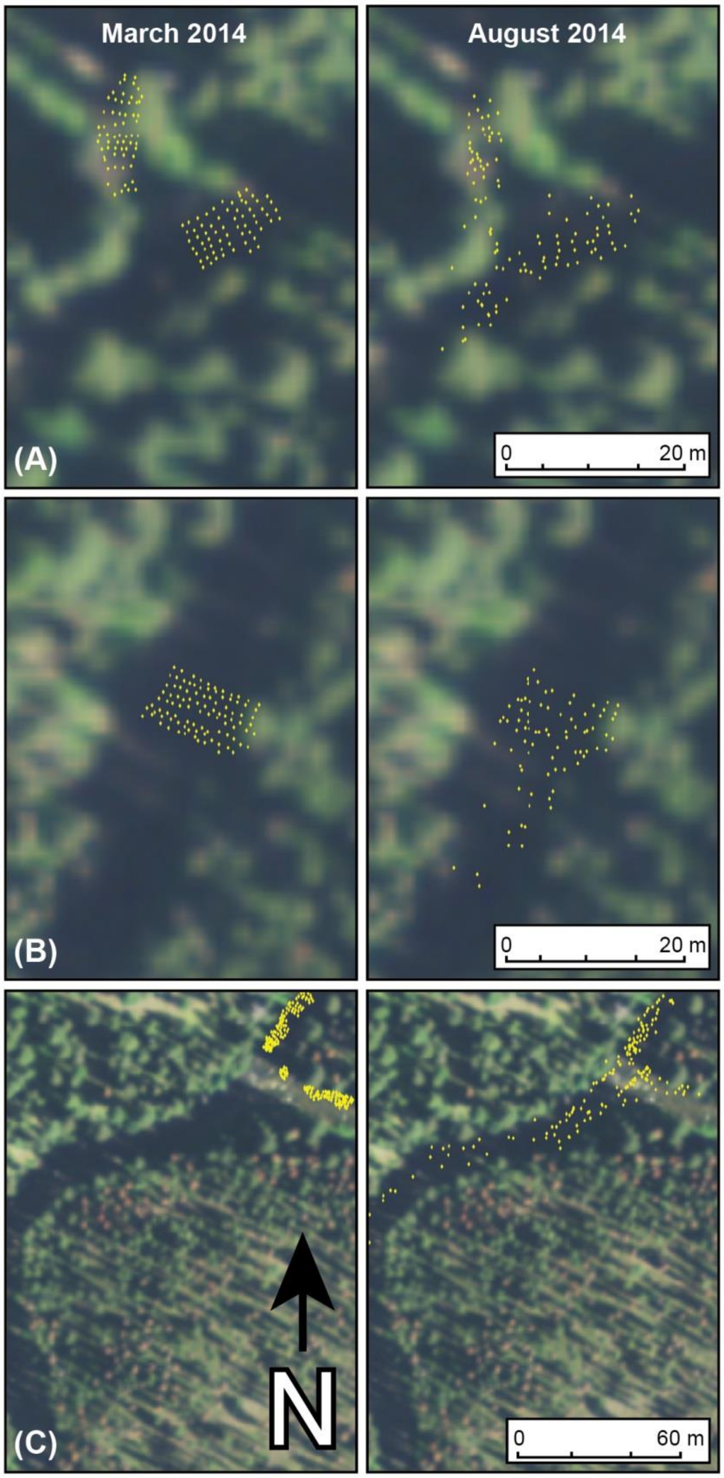

Figure 5: Tracer positions at initial installation (left) and following the 2014 flood (right) at (A~~a~~) the upper confluence, (B~~b~~) control reach, and (~~c~~C) lower confluence reaches.

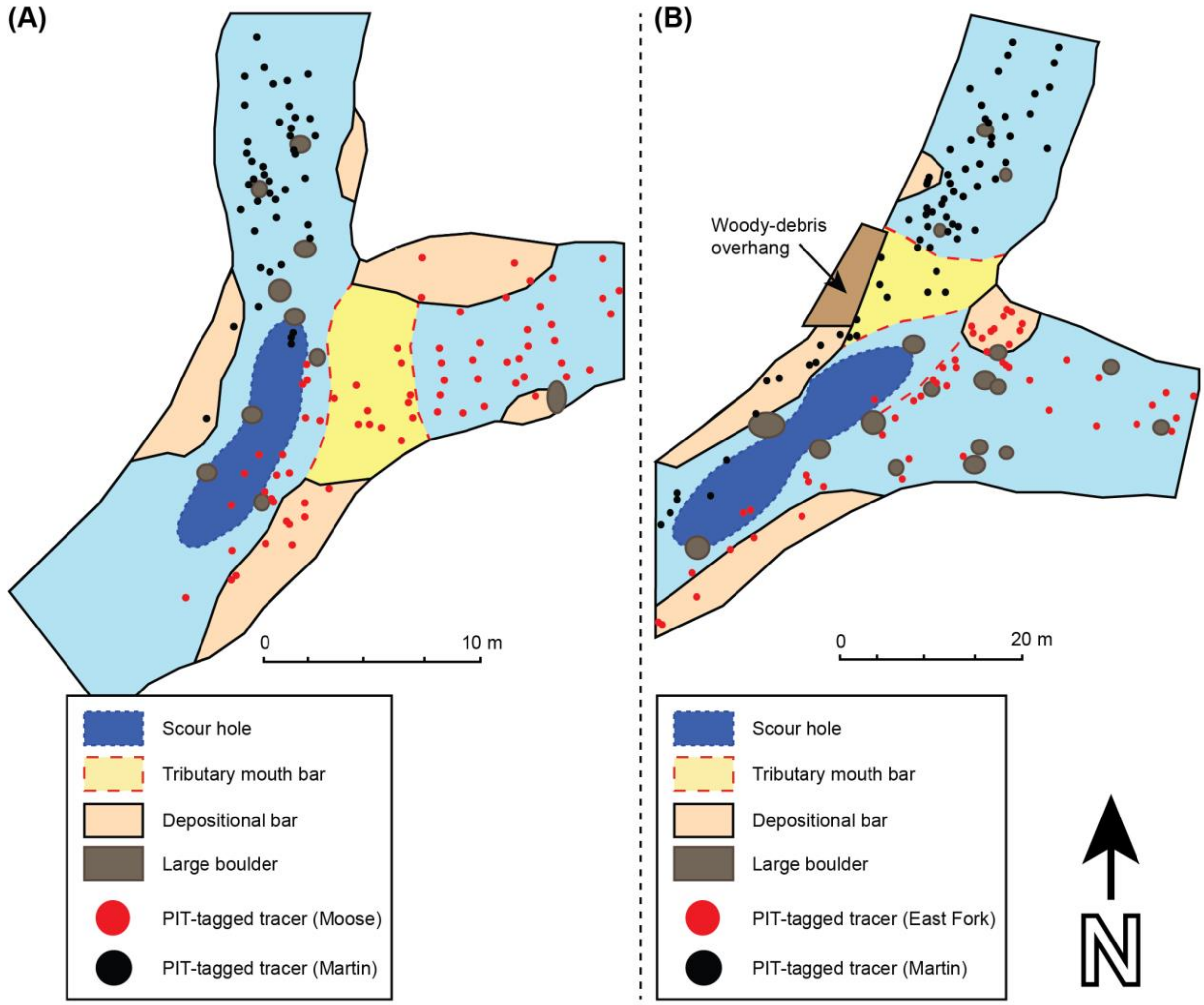

Figure 6: Digitized patch map of bedforms and tracer recovery positions at the (A) upper and (B) lower confluences.

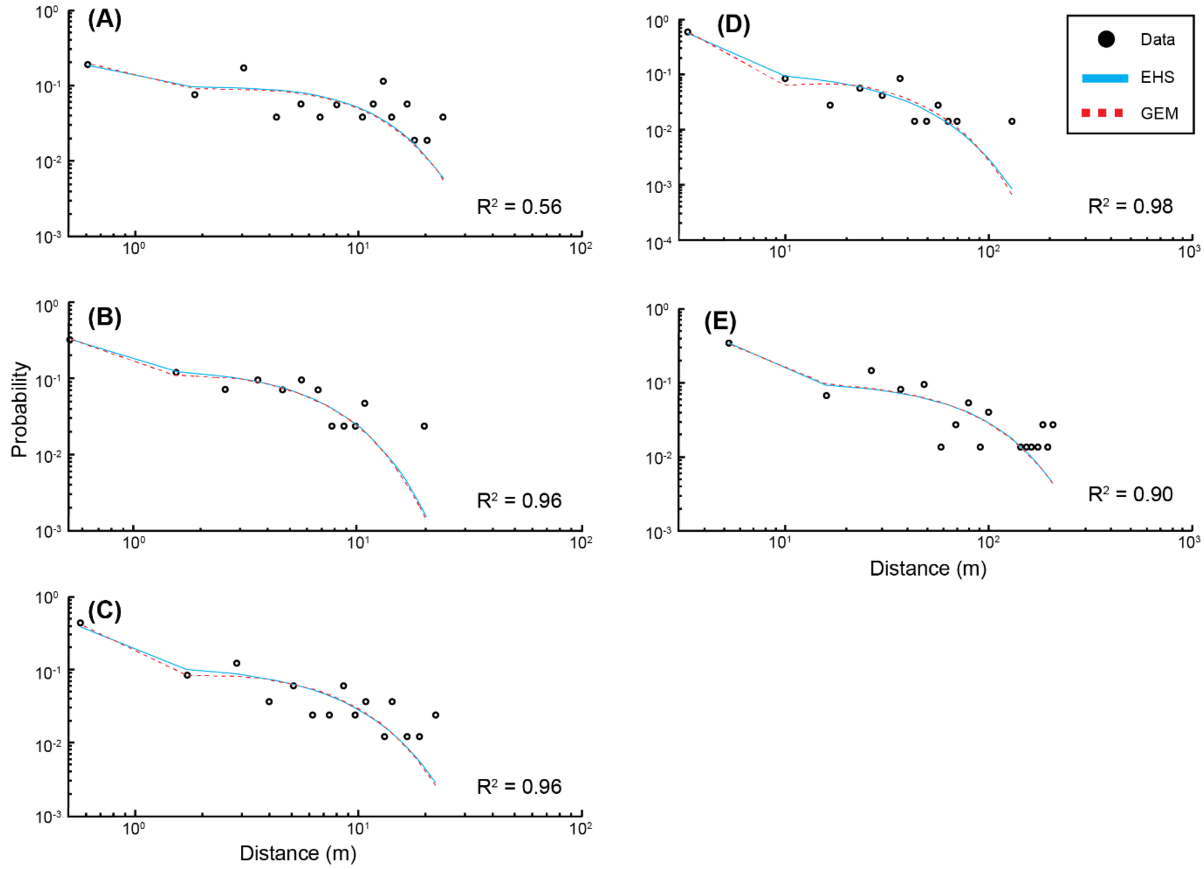

Figure 7: Einstein-Hubbell-Sayre (EHS) and Yang-Sayre (GEM) model fits for (A) Moose Creek, (B) Martin Creek (upper), (C) the control reach, (D) Martin Creek (lower), and (E) the East Fork Bitterroot River. R^2 fit differences between the two models were < 0.01, so we present their shared fit values here.

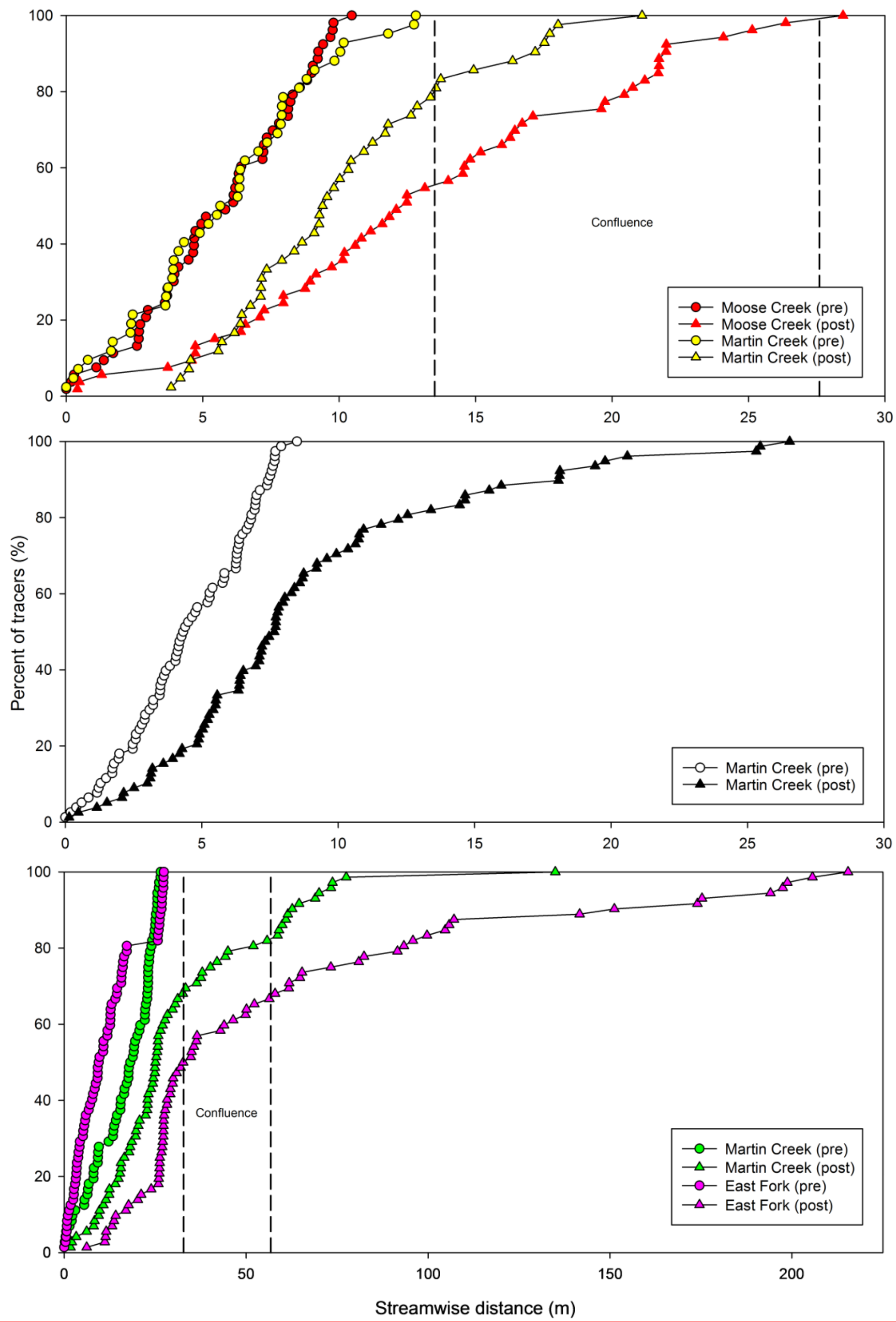

Figure 8: Spatial distribution of tracer positions at the time of initial deployment (pre) and after the 2014 flood (post) for (A) the upper confluence, (B) the control reach, and (C) the lower confluence. The confluence zones are bracketed with dotted vertical lines. Note the altered x-axis scale in (C).

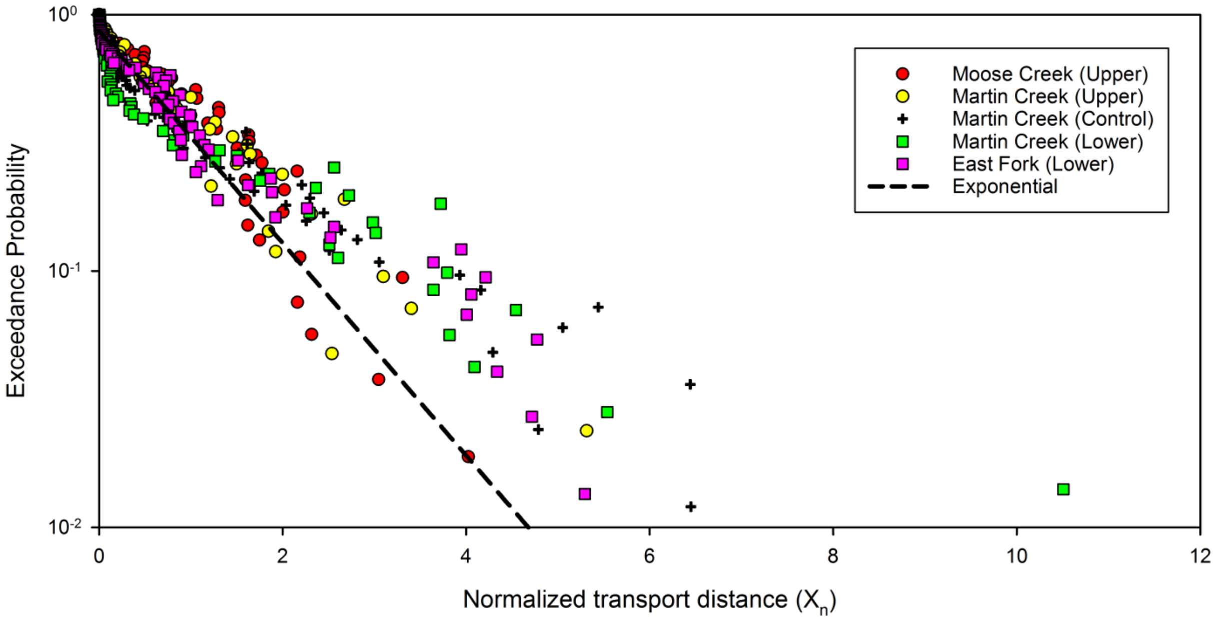

Figure 9: Normalized transport distances (X_n; Eq. 1)~~)~~ in all five study reaches~~ (Eq. 1)~~.

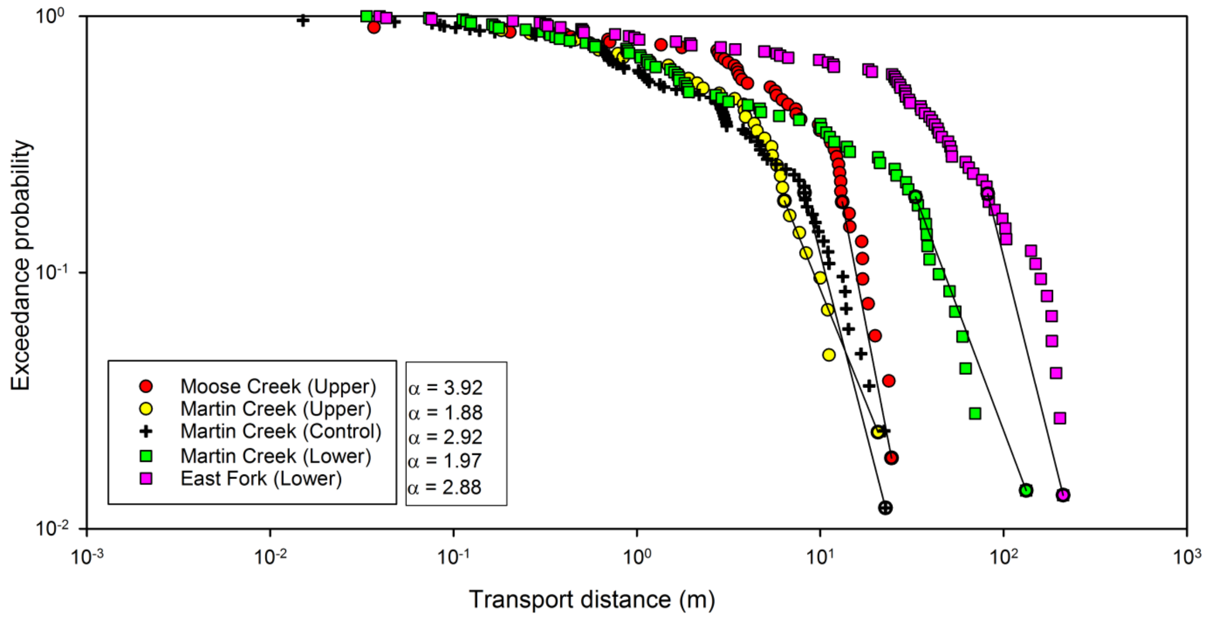

Figure 10: Cumulative exceedance distributions of travel distance for the upper confluence, lower confluence, and control reach.

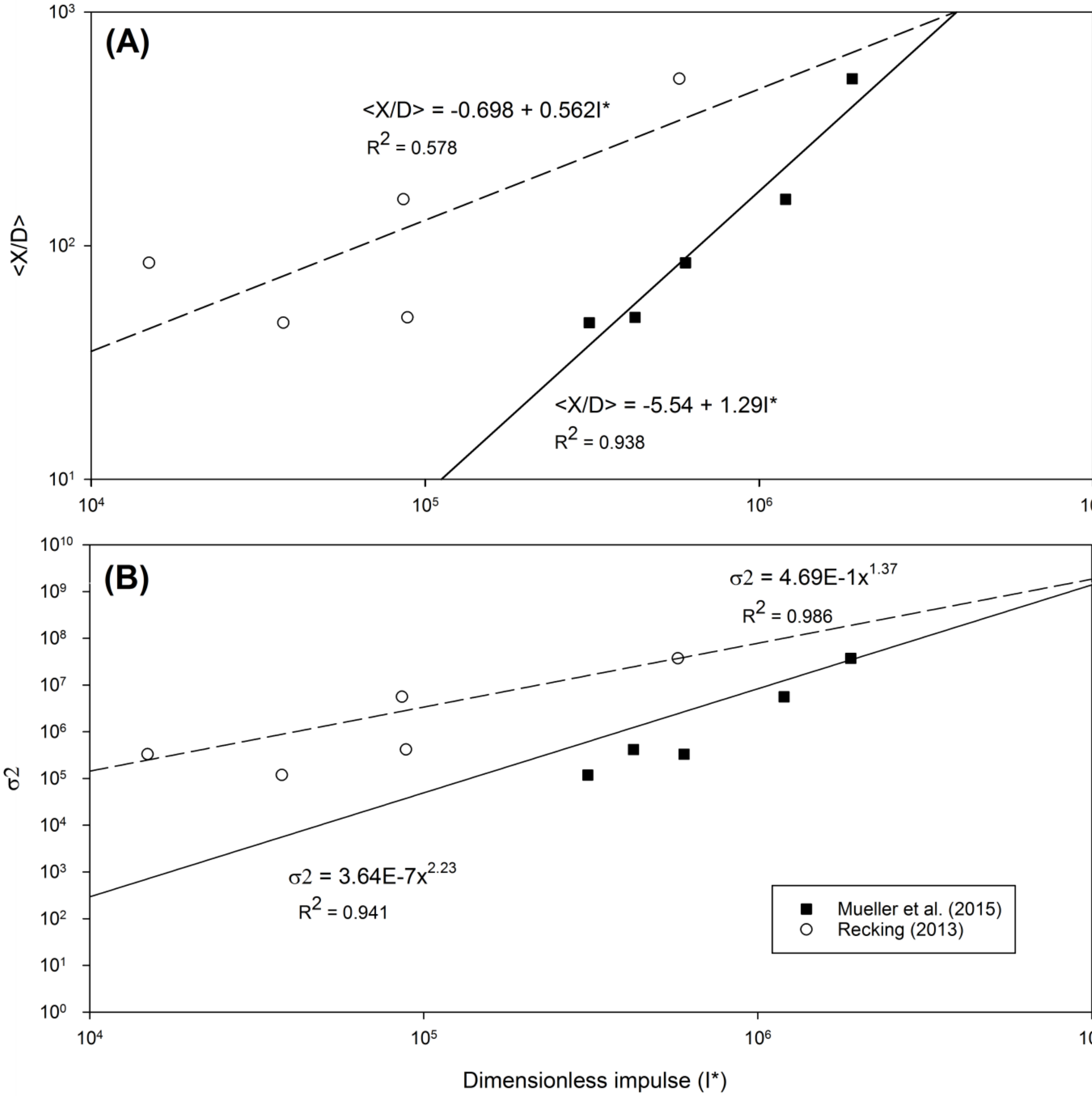

Figure 11: Linear and power-law relations between dimensionless impulse and (A) <X/D> and (B) σ^2.

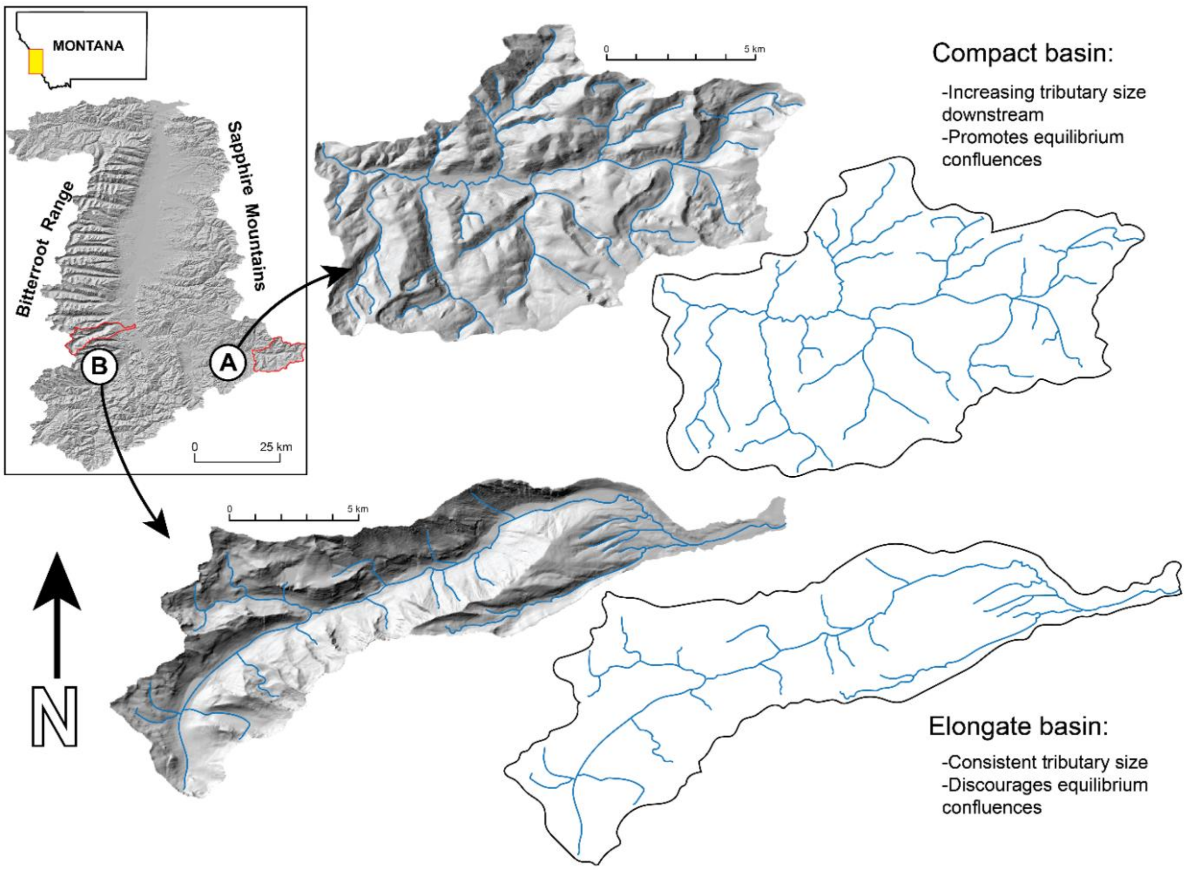

Figure 12: Typical basin shapes and tributary sizes in the (A) Sapphire Mountains (East Fork Bitterroot River) and (B) Bitterroot Range (Tin Cup Creek). These basins are of similar drainage area, but differ in lithology, erosional history, basin morphology, and potential sediment routing.